THE INHIBITION OF M-MLV AND HIV-1 REVERSE TRANSCRIPTASES BY POLYPHENOLS EXTRACTED FROM THE RESURRECTION PLANT *Myrothamnus flabellifolia* (Welw.)

KAMNG'ONA AROX WADSON

Thesis Presented for the Degree of

MASTER OF SCIENCE

In the Department of Molecular and Cellular Biology

UNIVERSITY OF CAPE TOWN

FEBRUARY 2008

PREFACE

This thesis was supervised by Associate Professor W. F. Brandt and Professor G. G. Lindsey. I hereby declare that this thesis, submitted for the degree of Master of Science in Molecular and Cell Biology at the University of Cape Town, is the result of my own investigation. The work done by others has been acknowledged accordingly.

Signed by candidate

KAMNG'ONA AROX WADSON

FEBRUARY 2008.

ACKNOWLEDGEMENTS

I would like to acknowledge GOD the almighty for keeping me in good health and for giving me the strength to carry on with this research work regardless of the difficulties I faced. My sincere gratitude also goes to my loving wife Mtisunge for her unwavering love and support in a number of ways. To my girls Juanita and Tamanda I say thank you. You guys were such an inspiration to me and you motivated me to work even harder. To my mum and late dad, thank you. Your love, care and support brought me this far.

I am greatly indebted to Associate Professor Wolf Brandt and Professor George Lindsey who worked tirelessly in their respective roles as principal supervisor and co-supervisor. As a young scientist, I consider it an honor to have been given an opportunity to tap from your immense intellectual knowledge in biochemistry.

My sincere appreciation also goes to Professor Chris Whiteley (Rhodes University, RSA) for personally sending me his publications, and my labmate Linah for her continued constructive criticisms. To my friends: Kevin, John, Peter, Leela, Andrew, Vanessa, Evan, Alexandra, Aderito, Erick, Catherine, lab 402, and the entire MCB department, many thanks for cheering me up every step of the way.

I am very thankful to NORAD and NRF for funding this study. Special mention goes to my employers, University of Malawi (College of Medicine) for securing and administering NORAD funds.

LIST OF ABBREVIATIONS

ADP	Adenosine diphosphate
ATP	Adenosine triphosphate
AZT	Azidothymidine
BSA	Bovine serum albumin
cDNA	complementary DNA
ctDNA	Calf thymus DNA
DHB	Dihydrobenzoic acid
DNA	Deoxyribonucleic acid
dsDNA	double stranded DNA
dATP	Deoxyadenosine triphosphate
dAMP	Deoxyadenosine monophosphate
dCTP	Deoxycytosine triphosphate
ddNTP	diDeoxynucleotide triphosphate
dGTP	Deoxyguanosine triphosphate
DMSO	Dimethyl sulphoxide
dNTP	Deoxynucleotide Triphosphate
dT	Deoxythymidine
dTMP	Deoxythymidine monophosphate
dTTP	Deoxythymidine triphosphate
EtBr	Ethidium Bromide
FC	Folin-Ciocalteau

HIV-1	Humman Immunodeficiency Virus type 1
HIV-2	Humman Immunodeficiency Virus type 2
HPLC	High Performance Liquid Chromatography
IC_{50}	50 % Inhibitory concentration
kDa	Kilodaltons
K_{cat}	Turnover number
K_i	Inhibition constant
K'_i	Apparent inhibition constant
K_m	Michaelis constant
K'_m	Apparent Michaelis constant
LDL	Low density lipoprotein
M	Molar
MALDI-TOF	Matrix Assisted Laser Desorption/Ionisation Time-of-Flight
M. *flabellifolia*	*Myrothamnus flabellifolia*
mM	Milli-Molar
µM	Micro-Molar
M-MLV	Moloney Murine Leukemia Virus
NNRTIs	Non-nucleoside reverse transcriptase inhibitors
NRTIs	Nucleoside reverse transcriptase inhibitors
NTP	Nucleotide Triphosphate
PVP	Poly[1-vinylpyrrolidone-2]
rA	Riboadenylic acid

RNA	Ribonucleic acid
RNAse	Ribonuclease
RT	Reverse transcriptase
SDS	Sodium dodecyl sulphate
TGQ	3,4,5 tri-*O*-galloylquinic acid
tRNA	Transfer RNA
V_{max}	Maximum velocity
V_o	Initial velocity

LIST OF FIGURES

LIST OF TABLES

TABLE OF CONTENTS

CHAPTER 2: POLYPHENOL EXTRACTION AND PURIFICATION

CHAPTER 3: ENZYMOLOGY OF REVERSE TRANSCRIPTASE

ABSTRACT

Polyphenols have been shown to exhibit anti-viral activity *in vitro*, making them a promising starting point for the development of HIV treatment drugs. The main objective of this thesis was to assess the inhibitory effect of polyphenols extracted from *Myrothamnus flabellifolia* (Welw.) on M-MLV and HIV-1 reverse transcriptases. The first part of the thesis was an attempt to isolate 3,4,5 tri-*O*-galloylquinic acid, the major polyphenol found in Namibian *Myrothamnus flabellifolia* plants. This polyphenol was successfully purified by column chromatography (Sephadex LH-20) and its purity was confirmed by HPLC and MALDI-TOF mass spectrometry. The second part of this thesis involved the development of a polymerase enzyme activity assay based on ethidium bromide fluorescence. A calibration curve for quantification of DNA was therefore prepared from the ethidium bromide fluorescence of Calf Thymus DNA. Results demonstrated that Calf Thymus DNA was a good standard for estimating the amount of cDNA synthesised during reverse transcription, thus enabling the monitoring of both M-MLV and HIV-1 reverse transcriptase activity. The reverse transcriptase activity assay was optimised using a poly (rA) template, an oligo $(dT)_{25}$ primer and dTTP as a substrate. It was observed that the rate of catalysis for M-MLV and HIV-1 RTs decreased with increase in the concentration of dTTP, which suggested substrate inhibition. A decrease in M-MLV RT activity with increased substrate concentration was found to be due to depletion of Mg^{2+} ions by dTTP. True substrate inhibition was however observed for HIV-1 RT, and analysis of the observed kinetics suggested the formation of an ineffective enzyme substrate complex with two substrate molecules binding to

HIV-1 reverse transcriptase. A Hill coefficient of one was obtained at low dTTP concentration and less than one at high dTTP concentration, suggesting zero and negative cooperativity respectively. The final part of this thesis tested the inhibitory effect of pure and crude polyphenol fractions on the activity of M-MLV and HIV-1 RTs. Results showed that all polyphenol fractions inhibited M-MLV and HIV-1 reverse transcriptase activity, with the highest inhibitory activity demonstrated by the fraction that contained pure 3,4,5 tri-*O*-galloylquinic acid. The 50 % inhibitory concentrations of 3,4,5 tri-*O*-galloylquinic acid was 0.5 μM for M-MLV RT and 34 μM for HIV-1 RT. Lineweaver-Burk plots showed that 3,4,5 tri-*O*-galloylquinic acid inhibited both enzymes non-competitively. Pure non-competitive inhibition was observed for M-MLV RT and mixed non-competitive inhibition for HIV-1 RT. Results showed that the binding of 3,4,5 tri-*O*-galloylquinic acid to M-MLV RT was irreversible, suggesting strong binding under the conditions tested. 3,4,5 Tri-*O*-galloylquinic acid, however, bound to HIV-1 RT reversibly. A comparison of catalytic efficiencies showed that M-MLV RT was more efficient than HIV-1 RT under saturating substrate concentrations with K_{cat} (min^{-1}) values of 11 ± 3 and 1.31 ± 0.02 respectively. M-MLV RT and HIV-1 RT were, however, equally efficient under limiting substrate concentrations with K_{cat}/K_m ($min^{-1}M^{-1}$) values of 1.1 ± 0.3 x 10^4 and 1.2 ± 0.2 x 10^4 respectively.

CHAPTER 1

GENERAL INTRODUCTION

1.1 The Plant *Myrothamnus flabellifolia*

Myrothamnus flabellifolia (*M. flabellifolia*) is a woody resurrection plant that survives long spells of drought during which it loses 95 % of its water content and retains most of its chlorophyll. It grows in various regions of southern Africa where it grows on shallow soils and rocky outcrops (Figure 1.1). It has an extensive root network system that penetrates rock crevices, thus making use of water trapped during rainy season (Sherwin et al., 1998, Viljoen et al., 2002, Moore et al., 2007).

Figure 1.1: Desiccated *M. flabellifolia* plant, growing on rocky area in Namibia

This plant has been reported to dehydrate its leaves to an air dried state, causing the leaves to fold in such a way changing the original green colour of the plant to brown. This condition is termed anhydrobiosis and has many detrimental effects such as irreversible damage to lipids, proteins, nucleic acids as well as the generation of reactive oxygen species (Kranner et al., 2002). Unlike most plants, *M. flabellifolia* is able to regain its original colour and shape once it is rehydrated (Figure 1.2).

Thus *M. flabellifolia* has the ability to maintain its physiological state under anhydrobiotic conditions as well as recover from the damage induced during transition from a desiccated to a rehydrated state. *M. flabellifolia* has been reported to retain a significant amount of chlorophyll in the dried state which enables it to rapidly recover once it is rehydrated (Kranner et al., 2002). Plants which are able to revive from their desiccation state are commonly known as desiccation tolerant or resurrection plants (Viere et al., 2003).

Dehydrated Rehydrated

Figure 1.2: *M. flabellifolia* in the dehydrated and rehydrated states

1.2 Medicinal use of *M. flabellifolia*

M. flabellifolia has a long history of use as a medicinal plant. It has been used to treat coughs, abdominal pains, kidney disorders as well as to sterilize wounds (Moore et al., 2007). Smoke from the burnt plant directed into the vagina has been used to treat uterine pain. Leaves have also been reported to treat gingivitis when chewed (Van Wyk and Gericke, 2000).

1.3 Constituents of *M. flabellifolia*

The leaves of *M. flabellifolia* have been reported to contain essential oils such as camphor and eucalyptol (Van Wyk and Gericke, 2000). These essential oils are thought to play a role in the healing properties of this plant (Viljoen et al., 2002). Recent studies have also shown that *M. flabellifolia* leaves contain a substantial amount of polyphenols (40 % by dry weight), the composition of which varied among plant samples from different geographical locations. The phenolics of Namibian plants, for instance, were shown to consist mainly of 3,4,5-tri-*O*-galloylquinic acid (Figure 1.7) whereas South African plant phenolics consisted of 3,4,5-tri-*O*-galloylquinic acid as well as higher molecular weight galloylquinic acids (Moore et al., 2005a, 2005b). Current research has focused on understanding the role that these polyphenols play in desiccation tolerance as well as on the healing properties of this plant

1.4 Polyphenols and their chemistry

Polyphenols are secondary metabolites found in the leaves and other parts of higher plants, and they usually consist of at least one aromatic ring with one or more hydroxyl groups and other substituents. Polyphenols are classified into several groups including amongst others the flavonoids and tannins (Baxter et al., 1997, Bennick, 2002).

1.4.1 Flavonoids

Flavonoids are one of the largest and most diverse groups of polyphenols. They are based on a heterocyclic ring structure that is synthesized from phenylalanine and polyketide (Hagerman, 2002). Flavonoids are further divided into two branches, namely

3-desoxyflavonoids (e.g. Flavone) and 3-hydroxyflavonoids (e.g. Flavonol) (Figure 1.3) (Bennick et al., 2002).

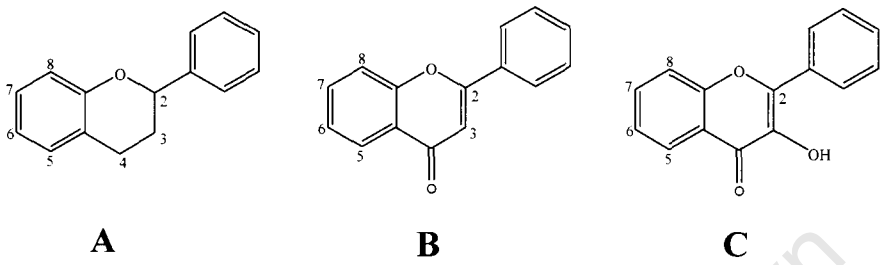

Figure 1.3: Structures of a basic flavonoid molecule (A) and two flavonoid branches: 3-desoxyflavonoid (B) and 3-hydroxyflavonoid (C)

1.4.2 Tannins

Tannins are plant polyphenolic secondary metabolites having molecular weights larger than 500 daltons, and are well known for their ability to precipitate proteins. Two classes of tannins are known: the condensed and the hydrolysable tannins (Bennick et al., 2002, Hagerman, 2002).

1.4.3 Condensed Tannins

Condensed tannins are formed by the polymerization of flavonoids through the formation of a covalent bond between the C-8 or C-6 of the terminal compound and C-4 of the flavan-3-ol extending compound (Figure 1.4) (Hagerman and Butler, 1981).

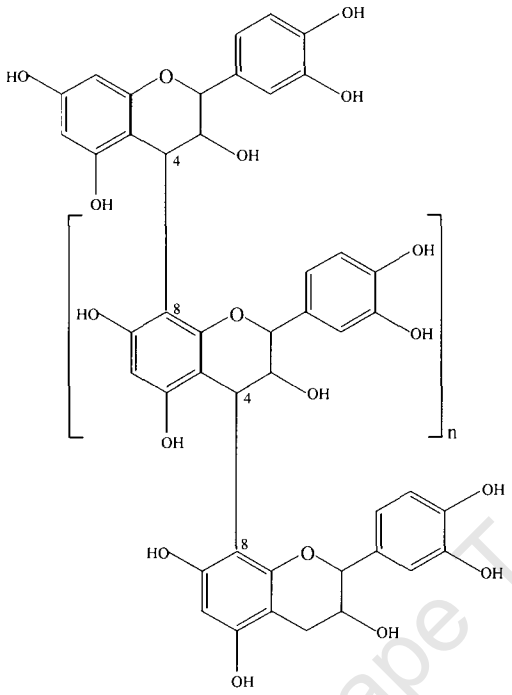

Figure 1.4: Basic structure of condensed tannins

The structure shows C8-C4 linkages and n can be equal to or above zero

Condensed tannins normally undergo oxidative cleavage in hot alcohols (acid butanol reaction) to produce an unchanged terminal unit and anthocyanidin pigments (Figure 1.5) from extender compounds. Thus condensed tannins are often called proanthocyanidins (Hagerman, 2002, Bennick, 2002).

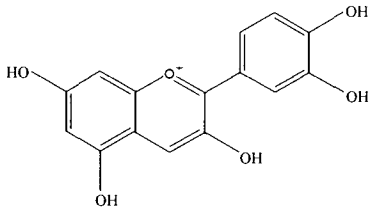

Figure 1.5: Basic structure of Anthocyanidins

1.4.4 Hydrolysable Tannins

Hydrolysable tannins are composed of a polyhydric alcohol, e.g. glucose or quinic acid, which is esterified to gallic acid or its dimer, hexahydroxydiphenic acid (Bennick, 2002, Makkar, 2003). Polymeric hydrolysable tannins are produced through oxidative cross-linkages or esterification of galloyl groups to other galloyl groups, resulting in the formation of depside bonds (Figure 1.6). Depside bonds are ester bonds that involve a phenolic hydroxyl rather than an aliphatic hydroxyl group (Hagerman, 2002, Bennick, 2003).

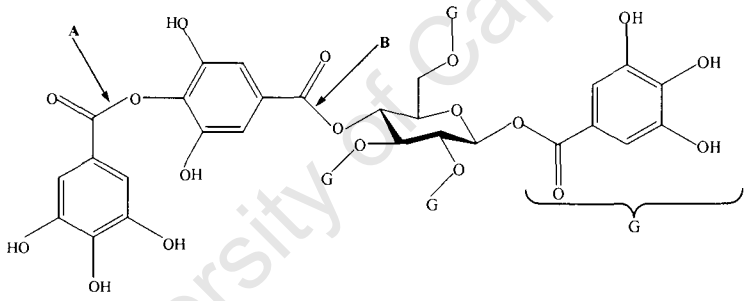

Figure 1.6: Basic structure of a hydrolysable tannin showing *meta*-depside (A) and ester (B) bonds

Examples of hydrolysable tannins include 3,4,5 tri-*O*-galloylquinic acid, which has been reported as the major polyphenol in the leaves of Namibian *M. flabellifolia* plants (Moore et al., 2005b). In this compound, galloyl groups form ester bonds with the hydroxyl groups of the central quinic acid molecule.

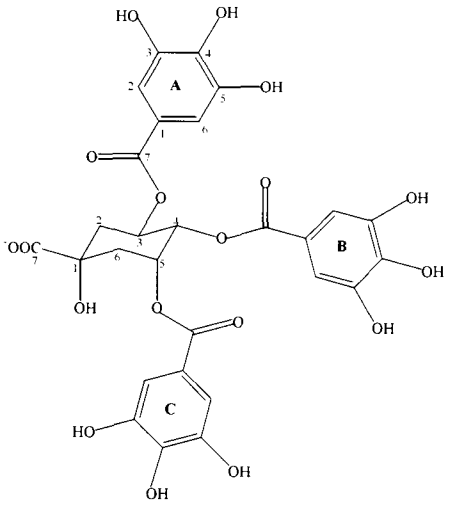

Figure 1.7: Structure of 3,4,5 tri-O-galloylquinic acid.

The major polyphenol compound in the Namibian resurrection plant, *Myrothamnus flabellifolia*

1.5 Biological functions of polyphenols

1.5.1 Role of polyphenols in plants

Polyphenols in plants are thought to protect against herbivores, act as antibiotics and protect against oxidative damage (Bennick et al., 2002). In this latter role, they are thought to not only chelate metal ions, thereby preventing metal ion-catalysed formation of free radicals but also to donate electrons to neutralize such radicals (Hagerman, 2002). Their anti-herbivorous activity is thought to be due to precipitation of salivary proteins which limits digestibility and results in an astringent taste, thus making the plant unpalatable (Bennick et al., 2002). Recently, polyphenols have also been proposed to protect plants from desiccation by maintaining the integrity of biological membranes, since they were able to protect the structural integrity of liposomes (artificial membranes) subjected to dehydration and subsequent rehydration (Moore et al., 2005b).

1.5.2 Role of polyphenols in human health

Consumption of foods that are rich in polyphenols has been associated with prevention of disease (Scalbert and Williamson, 2000). Widely published are the health benefits of consuming tea and red wine, both containing high concentrations of polyphenols (Rein et al., 2000, Khan and Mukhtar, 2007). Flavonoids, for instance, are able to donate electrons which neutralize reactive oxygen species such as superoxide anions, hydroxyl radicals and lipid peroxy radicals. These radicals oxidize low density lipoproteins (LDL) leading to an inflammatory disease, atherosclerosis (Shrikhande, 2000). Superoxide also

enhances platelet aggregation which is crucial in the development of diseases such as stroke (Rein et al., 2000).

1.5.3 The Polyphenol – Protein interaction

Polyphenols, particularly tannins, are well known for their ability to interact with proteins through hydrophobic as well as hydrogen bonding interactions. Hydrophobic interactions are thought to occur through the interaction between the galloyl ring of the polyphenol and the pyrrolidine ring face in the proteins (Murray et al., 1994). Hydrogen bonding, on the other hand, occurs through the interaction between the hydroxyl groups of the polyphenol with the peptide carbonyl group, which is strengthened by the alkyl substitution on the amide nitrogen adjacent to the carbonyl. This carbonyl group acts as a strong hydrogen bond acceptor (Hagerman and Butler, 1981). Polyphenols and protein interactions have been proposed to undergo a two step mechanism. Initially, polyphenols form soluble non covalent complexes with proteins. Further addition of polyphenols cross-links the peptides resulting in an insoluble complex (Charlton et al., 2002). Thus the molar ratio of tannin to protein seems to determine the solubility of the complex that is formed. In the gastrointestinal tract, where proteins are in excess, soluble complexes predominate.

The precipitation process can be reversible or irreversible depending on the conditions under which complexation occurs. The reversibility is tested by treating the precipitate with protein denaturants such as SDS. SDS has been reported to solubilise the precipitate formed by polyphenol-protein interactions under non-oxidizing conditions. Oxidation

favours the formation of stable covalent linkages within the polyphenol-protein complex which are resistant to denaturation (Chen and Hagerman, 2004).

Since proteins form a major part of most biochemical processes, the presence of tannins would affect these processes. It has been reported that protein digestibility is reduced in tannin rich foods due to the fact that tannins bind to digestive enzymes and the dietary proteins (Carbonaro et al., 1996). Polyphenols have also been reported to inhibit HIV reverse transcriptase, an enzyme that catalyses synthesis of cDNA from viral RNA (Nishizawa et al., 1989, Bokesh et al., 1996). Polyphenols also interfered with the *in vitro* production of plant cDNA via reverse transcriptase and the PCR amplification of DNA due to their inhibitory interaction with the DNA polymerases (Koonjul et al., 1999).

1.6 Reverse Transcriptase

Reverse transcriptases belong to a DNA polymerase super family and play an important role in the retroviral life cycle (Das and Georgiadis, 2004). Retroviruses are multifunctional enzymes possessing both the RNA- and DNA- dependent polymerase and RNase H activities. The polymerase activity is responsible for the conversion of the single stranded RNA/DNA genome into double stranded DNA. The function of RNase H is to degrade the RNA strand of the RNA-DNA hybrid which is an intermediate in the retroviral replication process (Telesnitsky and Goff, 1993). *In vivo*, reverse transcription is initiated by the binding of tRNA to the primer binding site of the template, a process which is reportedly characterized by virus-specific interactions (Lanchy et al., 1996). Reverse transcriptases have five domains: fingers, palm, thumb, connection and RNase H. The overall shape of these domains is thought to resemble the shape of the right hand, hence the nomenclature (Das and Georgiadis, 2004). The DNA and RNase H catalytic sites lie in separate domains which are linked within the same polypeptide (Telesnitsky and Goff, 1993). Specific examples of enzymes in the RT DNA polymerase super family include the M-MLV and HIV-1 reverse transcriptases. M-MLV RT has a number of important applications in molecular biology such as cDNA synthesis due to its relative low cost. HIV-1 RT is an important enzyme in the life cycle of HIV infection (Figure 1.8) as it is responsible for converting a single stranded viral RNA to cDNA, which is later integrated into the host chromosomal DNA.

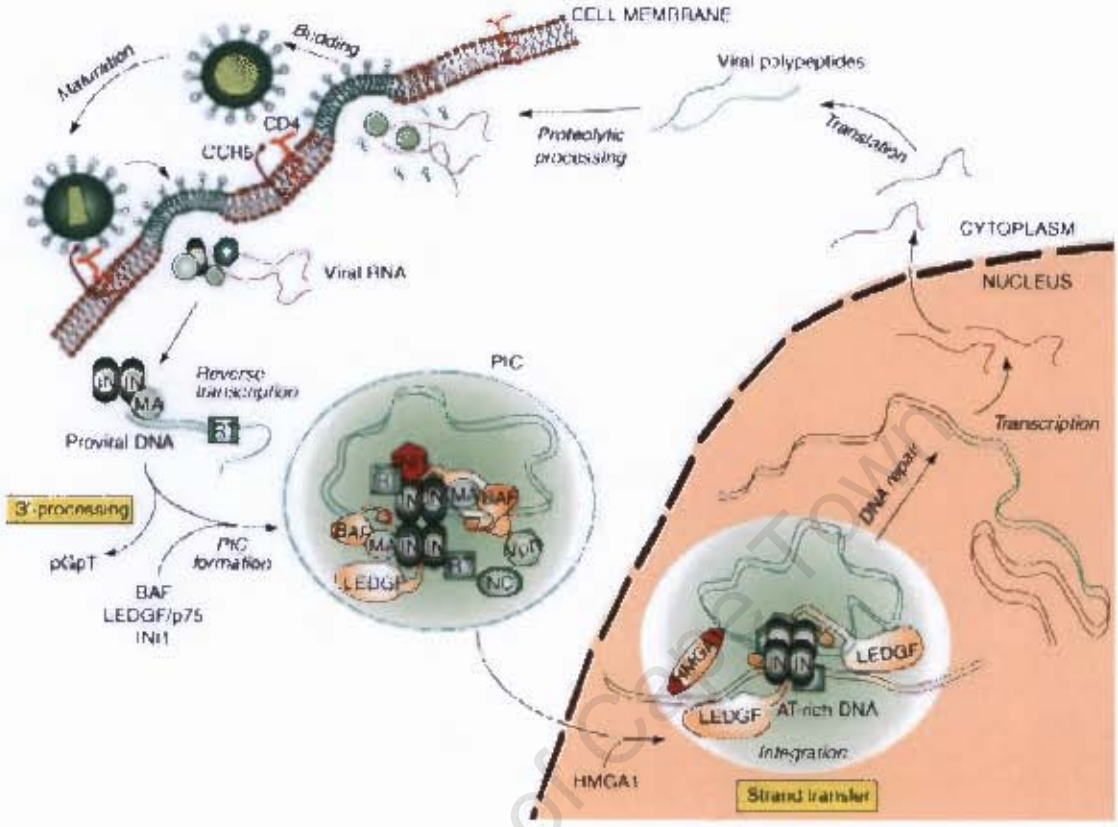

Figure 1.8: Schematic representation of the HIV-1 replication cycle (Marchand et al., 2006)

The HIV-1 virus initially binds to the cell CD-4 receptor and CCR5 co-receptor and releases the viral RNA into the cytoplasm. HIV-1 RT produces cDNA from the viral RNA which is transferred into the nucleus and then integrated into the chromosomal DNA by HIV-1 integrase. New viral DNA particles are produced through the normal transcription and translation processes of the chromosomal DNA.

1.6.1 M-MLV and HIV-1 RT Crystal Structures

Although RT enzymes exhibit similar catalytic functions, their structures are reported to be very different (Fig 1.9-10). All enzymes in the RT super family are monomeric except for HIV-1 RT which is heterodimeric (Das and Georgiadis, 2004). M-MLV RT consists of 671 amino acid residues with a molecular weight of approximately 75 kDa, and has all five domains located on its single sub-unit. HIV-1 RT has two subunits, p66 and p51, with molecular weights of 66 and 51 kDa respectively. These two subunits have four domains in common; the fifth, RNase H domain, is located on the p66 sub-unit. The polymerase activity of HIV-1 RT is located on the p66 subunit. (Huang et al., 1998).

1.6.2 M-MLV and HIV-1 RT p66 sub-unit

A comparison of the crystal structure for M-MLV and HIV-1 RT p66 using the highly conserved region in the palm domain highlights some important similarities and differences. The important similarity is that all five domains that are present on the M-MLV RT enzyme (Figure 1.9A) are located on the HIV-I RT p66 subunit. A notable difference is that rotation angles of 18° and 70° relative to the M-MLV RT active site were required to overlay the thumb and the connection domains of M-MLV RT respectively onto similar domains on the HIV-1 RT p66 sub-unit (Figure 1.9B) (Das and Georgiadis, 2004).

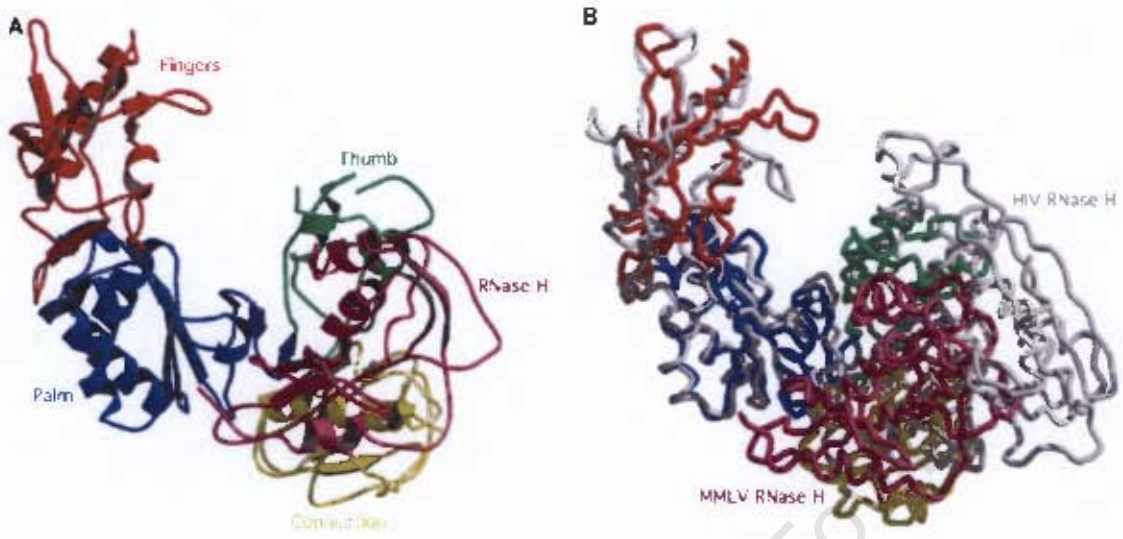

Figure 1.9: Crystal structures of M-MLV RT (A) and an overlay of M-MLV and HIV-1 RT p66 sub-unit structures (B). HIV-1 RT p66 sub-unit structure is shown in gray (Das and Georgiadis, 2004).

1.6.3 M-MLV and HIV-1 RT Thumb and Connection domains

The thumb domain is reported to play a crucial role in binding to the substrate and is also thought to act as a minor groove binding track which enables substrate translocation during polymerization. The residues involved in this binding site have not been conserved. Homologous residues Q258, G262, W266 in HIV-1 RT have been substituted by R298, E302, T306 respectively in M-MLV RTs. The thumb domains of the two enzymes are reported to have a similar folding pattern (Figure 1.10A), but do not fit perfectly when overlaid.

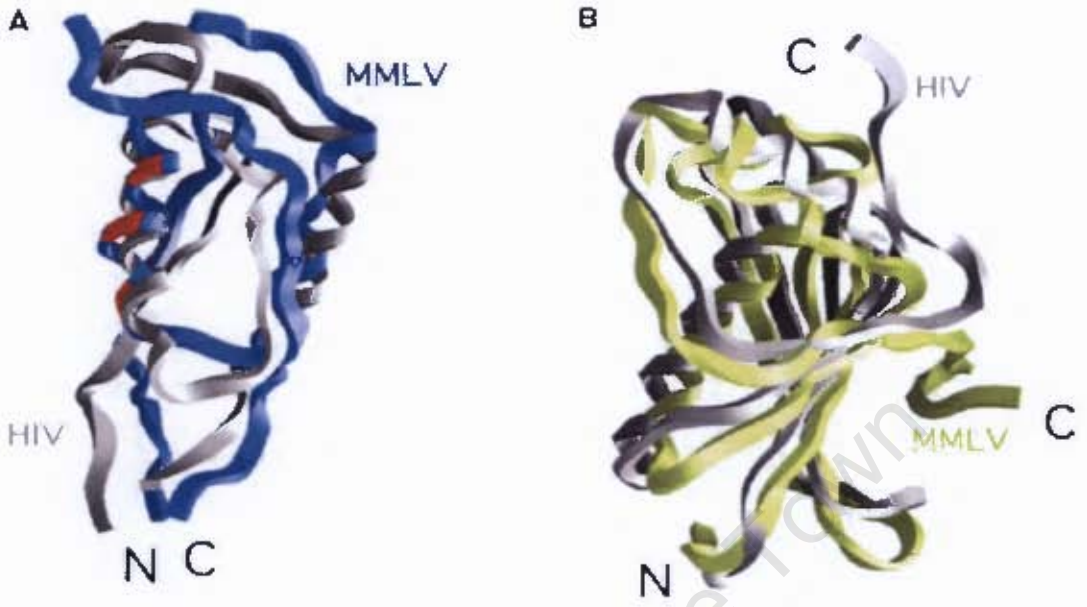

Figure 1.10: An overlay of crystal structures of the thumb domain (A) and the connection domain (B) for M-MLV and HIV-1 RTs (Das and Georgiadis, 2004)

The connection domains for both M-MLV and HIV-1 RT are also reported to have similar folding patterns, but fitted poorly when overlaid (Figure 1.10B). It has also been reported that the connection domain is linked directly to the RNase H domain in HIV-1 RT, whereas in M-MLV RT the polypeptide that links the two domains proceeds in the opposite direction and has an additional 32 amino acid residues (Das and Georgiadis, 2004).

1.6.4 M-MLV and HIV-1 RT sequence alignment

Sequence alignments demonstrated that secondary structures in the two enzymes occur at similar positions, although they differ in length (Figure 1.11). There is also greater sequence identity for the fingers and palm domains than for the connection and RNase H domains. M-MLV RT was observed to have smaller insertions such as residues 328 – 333

in the thumb domain and residues 473 -504 between the connection and RNase H domains that were absent in HIV-1 RT.

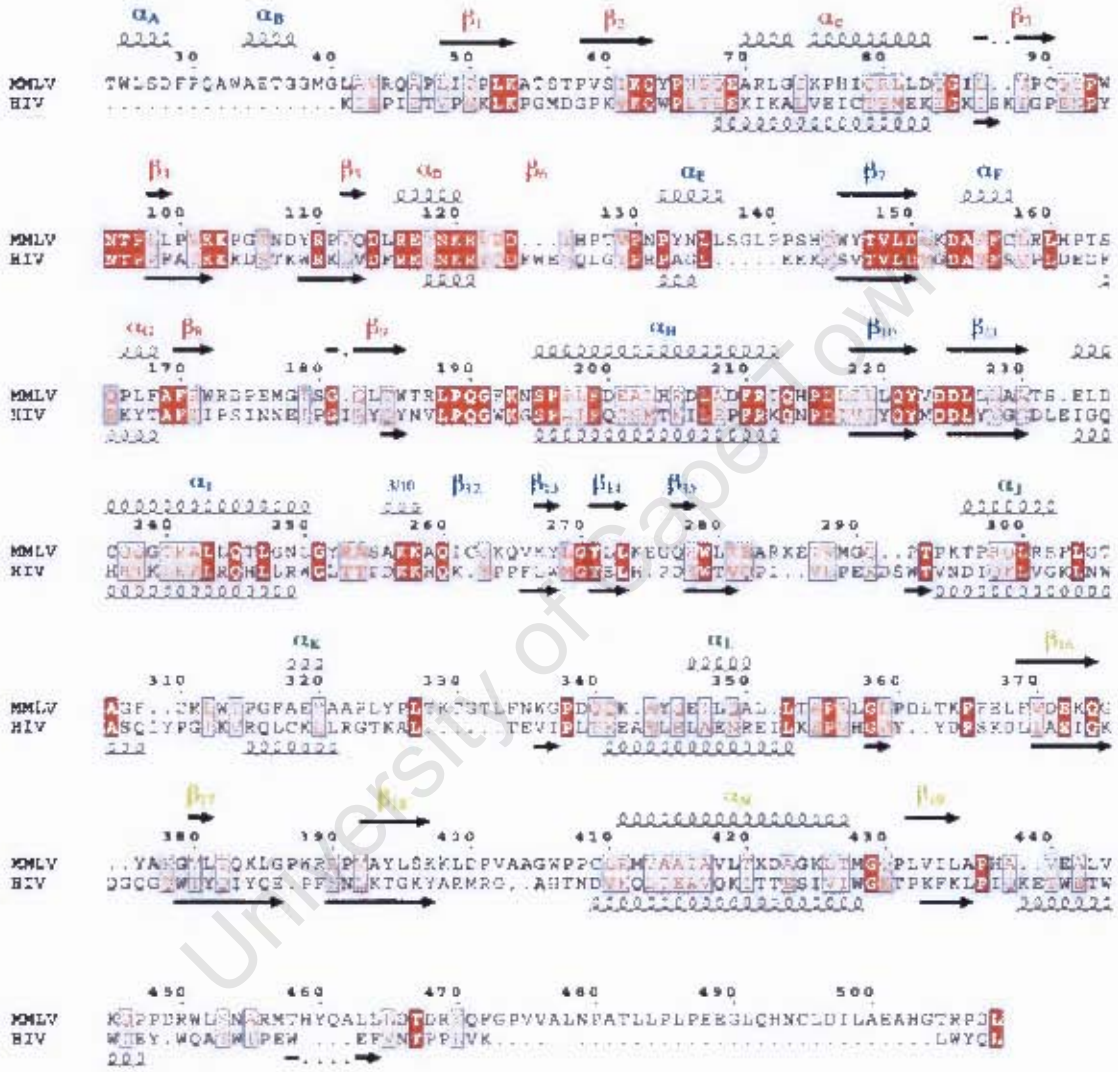

Figure 1.11: Sequence alignment of MMLV RT with HIV-1 RT based on crystal structure (Das and Georgiadis, 2004).

The colors for β strands and α-helices correspond to the colors of domains as shown in Figure 9A.

1.7 General mechanism of the polymerase reaction

There are a series of steps involved in the incorporation of dNTPs into the primer-template complex by DNA polymerases. Initially, the enzyme is thought to form a binary complex with the primer-template complex in an open conformation state. This open state allows further binding of the complementary dNTPs downstream of the 3′ - terminal primer nucleotide resulting in the formation of an open ternary complex. At this point the open ternary complex is changed to a closed ternary complex, which ensures coordination between the 3′-oxygen atom and the α-phosphorous of the dNTP through deprotonation. When the chemical reaction is complete, the enzyme completes its cycle of conformational changes by going back to an open state so as to allow release of pyrophosphate and to continue with the next dNTP incorporation (Yang et al., 2004, Oelschlaeger et al., 2007).

1.7.1 The role of magnesium ions in polymerization reaction

The mechanism of the polymerase reaction has been reported to occur through the involvement of two metal ions, and in the case of reverse transcriptase, two divalent magnesium ions (Yang et al., 2004). The first magnesium ion is bound to the nucleotide α-, β-, and γ-phosphate oxygen atoms and is brought into the enzyme active site by the incoming complementary dNTP. This ion is also thought to facilitate the release of pyrophosphate from the active site (Yang et al., 2004, Goldschmidt et al., 2006). The second magnesium ion has been reported to bind to the three catalytic aspartate residues and the α- phosphate of the incoming dNTP (Goldschmidt et al., 2006). This coordination is responsible for the nucleophilic attack of the primer 3′-OH on the

α- phosphate of the dNTP (Yang et al., 2004). A crystal structure of the HIV-1 RT catalytic complex bound to the template/primer complex and ddNTP has been reported (Figure 1.12A). The structure of the active site is shown in Figure 1.12B. This structure clearly shows the positions of the two Mg^{2+} ions, emphasizing the importance of Mg^{2+} ions in the polymerization reaction (Huang et al., 1998).

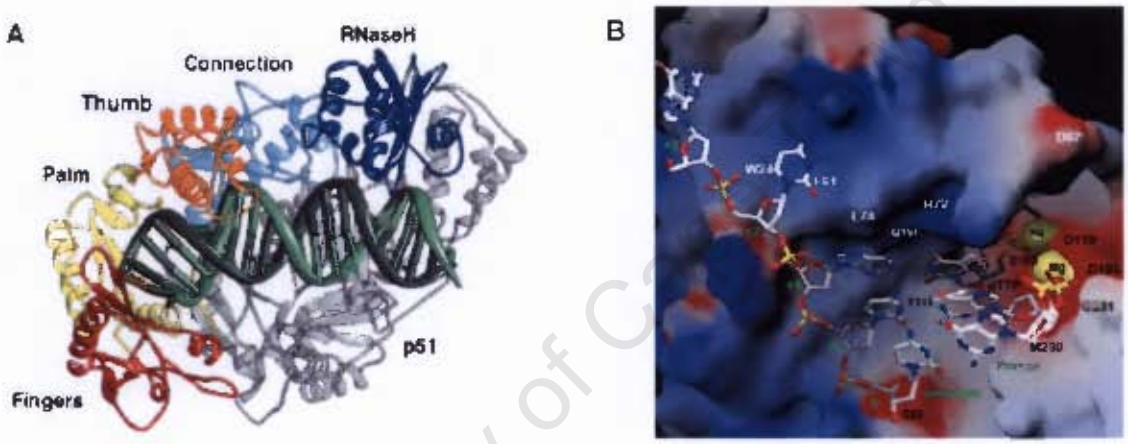

Figure 1.12: The general structure HIV-1 RT catalytic complex (A) and its active site (B) (Huang et al., 1998).

The general structure (A) shows the p66 subunit in colour and the p51 subunit in gray. The DNA template strand is shown in green. The active site (B) shows the background of the dNTP pocket formed by the fingers, palm and thumb domains in an appropriate conformation. The enzyme surface is shown in red for negative and blue for positive electrostatic potentials. The primer, template and dNTP are in stick representation whereas magnesium ions are presented as yellow spheres

1.8 Enzyme Inhibition

Enzyme inhibition refers to a reduction in the activity of an enzyme in the presence of other compounds. Knowledge of enzyme inhibition is crucial to the understanding of enzyme specificity as well as metabolic pathways (Whiteley, 2000). Enzyme inhibition is divided into two major classes, namely reversible and irreversible inhibition. Reversible inhibition is temporary and involves weak non-covalent interactions between the inhibitor and the enzyme. Irreversible inhibition is permanent and involves strong covalent interactions between the inhibitor and key amino acid residues of the enzyme, consequently decreasing the effective enzyme concentration (Garrett and Grisham, 2005). Further classification of enzyme inhibition is based on whether the inhibitor binds the enzyme at an active site or allosterically. Inhibition is competitive if the inhibitor binds to the active site and competes with the substrate, i.e. the inhibitor binds to the free enzyme only and its kinetics reveal an increase in K_m and no change in maximal velocity (V_{max}) values. In other cases, the inhibitor binds to a site on the enzyme other than the active site, in which case it is able to bind both the free enzyme and the enzyme substrate (ES) complex. This is known as non-competitive inhibition because the enzyme does not compete with the enzyme for binding to the active site. The K_m remains unchanged but the maximum enzyme velocity (V_{max}) is reduced. Finally, some inhibitors bind to the enzyme substrate (ES) complex only. This is known as un-competitive inhibition and the kinetics reveal changes in both K_m and V_{max} values (Garrett and Grisham, 2005).

1.8.1 The role of enzyme inhibition in biological systems

Enzyme inhibition plays an important role in the regulation of biological systems (Oliver and Shenolikar, 1998) as well as in chemotherapy (Maggi et al., 2000). Naturally, plants and animals have been reported to use poisons as a means of protecting themselves from predators. Many of these poisons function as enzyme inhibitors. In chemotherapy, most drugs function by inhibiting enzymes that are crucial in the pathways of both diseases (Cushman and Ondetti, 1995) and pathogenic organisms. Enzyme inhibitors also play an important role as insecticides, herbicides as well as disinfectants (Nomura et al., 2005).

1.8.1.1 Regulation of metabolic pathways

Most cellular processes are mediated by enzymes. These processes are well regulated to ensure normal metabolism, and this is achieved by controlling enzyme activity (Garrett and Grisham, 2005). *In vivo*, enzyme activity can be regulated by the concentration of metabolites such as substrates and products. If regulation of enzyme activity occurs through the involvement of hormones or nervous stimulation, it is known as extrinsic control. If it proceeds without any external influence, it is termed intrinsic. Glycolysis is one example of a metabolic process that is regulated through enzyme inhibition. In one of the glycolytic pathway steps, D-fructose 6-phosphate is converted to D-fructose 1,6-bisphosphate by phosphofructokinase in the presence of ATP. High ATP concentrations have been reported to inhibit the activity of phosphofructokinase, thus regulating the whole pathway (Price and Stevens, 1999).

1.8.1.2 Role in Chemotherapy

Enzyme inhibitors have a long history of use as chemotherapeutic agents (Szedlacsek and Duggleby, 1995). Viagra, a drug that is used to remedy erectile dysfunction, functions by inhibiting cGMP specific phosphodiesterase type 5, an enzyme that degrades the signaling molecule cyclic guanosine monophosphate (Maggi et al., 2000). Equally important is the role that enzyme inhibitors play in the treatment of HIV-AIDS. In the life cycle of HIV infection (Figure 8), there are a number of drug targets that can be used to reduce the infection such as prevention of the binding of HIV-1 gp120 to CD4 receptors as well as enzyme mediated processes. To date, the approved treatment of HIV infection has been restricted to two of the three target enzymes, HIV-1 reverse transcriptase (HIV-1 RT) and HIV-1 protease (HIV-1 PR) (Notka et al., 2004, Marchand et al., 2006). The above illustrate the important role played by enzyme inhibitors in the control of pathogens and often form the basis of new drug discoveries.

1.9 HIV-1 Reverse Transcriptase as a target for Anti-HIV drugs

HIV-1 RT plays a crucial role in the replication cycle of HIV. In general, RTs are not required for normal metabolic processes in the host cell, and are thus important targets for antiviral therapy (Sarafianos et al., 1996, Pelemans et al., 2000). The current antiviral drugs are targeted at the RT polymerase and not the RNase activity (Huang et al., 1998). Inhibitors of RT catalysed polymerization are divided into two groups: nucleoside RT inhibitors (NRTIs) and non-nucleoside RT inhibitors (NNRTIs). NRTIs are substrate analogues that act by chain termination (Ren et al., 2001, Pata et al., 2004). The first drug to be approved for HIV therapy was AZT, a nucleoside inhibitor. This drug was, however, reported toxic to the host and complete inhibition of HIV replication was not attained (Merluzzi et al., 1990). NNRTIs constitute compounds with a wide range of chemical formulae and are generally very specific for HIV-1 RT (Smerdon et al., 1994, Ren and Stammers, 2005). These compounds inhibit HIV-1 RT by binding at an allosteric site, resulting in conformational changes that displace catalytic aspartate residues in the active site (Ren et al., 2001, Pata et al., 2004). Nevirapine is an example of a first line non-nucleoside inhibitor and, like most NNRTIs, suffers from a rapid selection of resistant HIV strains. This resistance has generally been associated with Tyr 181 and Tyr 188 mutations within the NNRTIs binding pocket (Ren and Stammers, 2005).

1.9.1 Crystal structure of HIV-1 RT bound to a non-nucleoside inhibitor

NNRTIs have been reported to bind to the same hydrophobic pocket which results from the displacement of the polypeptide portion between the palm and thumb domains, in

close proximity to the active site. This is consistent with the observation that mutant RTs resistant to any one NNRTIs are also resistant to all NNRTIs (Smerdon et al., 1994). The hydrophobic pocket is only available on the p66 subunit and, as expected, NNRTIs do not bind to the p51 subunit (Huang et al., 1998). Crystal structures of HIV-1 RT bound to different NNRTIs such as Efavirenz, Delaviridine and Nevirapine have been reported (Kohlstaedt et al., 1992, Pata et al., 2004). Nevirapine has been shown to bind close to the β-hairpin between strand 9 and 10 in the p66 palm sub- domain (Figure 1.13A). The amino acid residues in the hydrophobic pocket in contact with Nevirapine are shown in Figure 1.13B. The most important mutations that confer resistance to NNRTIs occur at Tyr-181 and Tyr-188 shown in bold font (Smerdon et al., 1994).

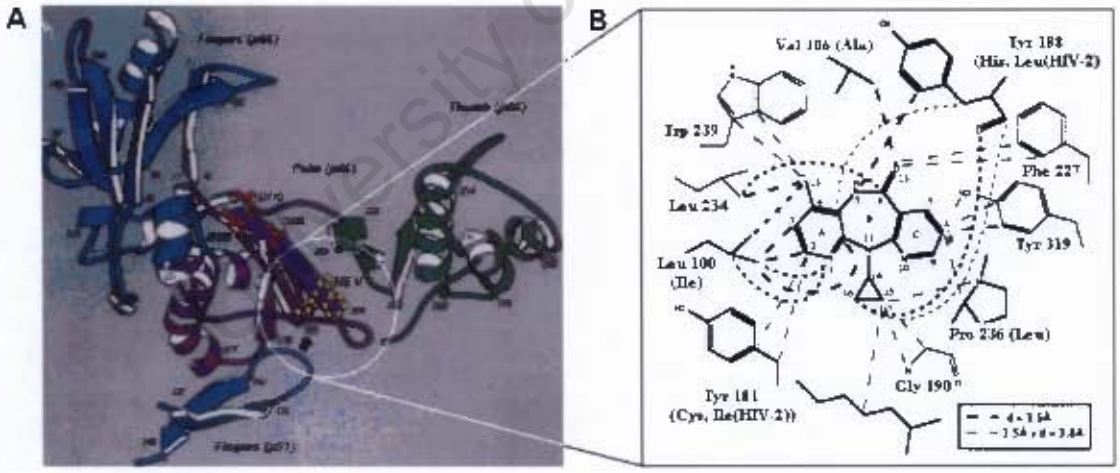

Figure 1.13: Crystal structure of HIV-1 RT p66 subunit bound to Nevirapine (shown in yellow) (A) and a schematic representation of amino acid residues in contact with Nevirapine (B) (Smerdon et al., 1994)

1.10 Objectives

1.10.1 Main objective

The main objective of this project was to investigate the inhibition of M-MLV RT and HIV-1 RT activity by polyphenols extracted from the resurrection plant *Myrothamnus flabellifolia*

1.10.2 Specific objectives

1.10.2.1 Extraction, purification and characterization of polyphenols from *M. flabellifolia*

1.10.2.2 Development of a reverse transcriptase activity assay based on ethidium bromide fluorescence

1.10.2.3 Investigating the inhibition of M-MLV RT activity by polyphenols from *M. flabellifolia*

1.10.2.4 Investigating the inhibition of HIV-1 RT activity by polyphenols from *M. flabellifolia*

CHAPTER 2

POLYPHENOL EXTRACTION AND PURIFICATION

2.1 INTRODUCTION

Polyphenols can be extracted from both dry and fresh plant material. The sample is initially homogenized by grinding. Liquid nitrogen is often used when working with fresh material so as to facilitate the homogenization process. The use of liquid nitrogen also ensures that temperatures are kept as low as possible during grinding since high temperatures lead to polyphenol degradation (Makkar, 2003).

Extraction of polyphenols from plant materials is performed by several methods, namely solvent extraction, solid phase extraction or supercritical fluid extraction. Solvent extraction separates soluble polyphenols from the sample material and is usually accompanied by sonication or microwave heating to make cell walls more permeable to the extracting solvent. Solid phase extraction may utilize hydrophobic cartridges which are employed to remove polyphenols from the solvent. It is sometimes used in combination with solvent extraction. Supercritical fluid extraction operates on the same principles as solvent extraction. The difference is that supercritical fluid extraction takes into account the properties of both gases and liquids for extraction. Methanol is often used as a solvent for extracting polyphenols although other solvents such as acetone, ethyl acetate and ethanol have also been reported (Escribano-Bailon and Santos-Buelga, 2003).

Estimation of polyphenol concentrations in the extract is now generally performed using Folin-Ciocalteau reagent (Hagerman, 2002). It is based on the reduction of Mo^{3+} to Mo^{2+} ions in an alkaline environment resulting in a yellow to blue color change, which is quantitated spectrophotometrically (Mozetic et al., 2006). The reducing capacity of a given polyphenol extract is compared to a given standard such as gallic acid (Hagerman, 2002) and polyphenol concentrations are then expressed as equivalents of the standard used.

The purification of polyphenol extracts is often performed using column chromatography. Sephadex LH-20 has been reported to be an ideal matrix for separating natural products such as plant phenolic compounds (Pharmacia Handbook, Amarowicz et al., 2003). Separation of the phenolic compounds on Sephadex LH-20 is achieved through both adsorption and size exclusion chromatography (Amarowicz et al., 2003, Seger et al., 2006). Tannins dissolved in alcohol are reported to bind to Sephadex LH-20, whereas low molecular weight phenolics do not (Hagerman, 2002). Elution of bound phenolics from the column is achieved by using solvents such as methanol, acetone or ethanol, and quite often aqueous mixtures of these solvents (Kantz and Singleton, 1990, Amarowicz et al., 2003, Seger et al., 2006).

The purity of polyphenol preparations can be assessed by analytical HPLC. Reverse phase HPLC for instance utilizes a hydrophobic C_8 or C_{18} alkyl bonded stationary phase and mobile phases of varying polarity. Compounds are generally eluted in-order of decreasing polarity (Escribano-Bailon and Santos-Buelga, 2003). Additional characterization and identification of purified compounds can be achieved using

MALDI-TOF mass spectrometry. MALDI-TOF.MS works by ionizing and transferring the sample (embedded in a solid matrix) from a solid state into a gas state. The matrix aids the solid-gas phase transition and facilitates the ionization of the sample. A laser beam supplies energy for this transformation. The ions are separated based on their mass to charge ratio with lighter molecular ions moving faster and hence detected earlier than heavier ions. MALDI-TOF has several advantages, which include the production of mainly single charged molecular ion for each parent molecule and the high precision with which it detects high molecular weight compounds (Reed et al., 2005).

2.2 MATERIALS AND METHODS

2.2.1 Plant material

M. flabellifolia plant material was collected in Namibia at the edge of the central highlands and the coastal Namib Desert plains (GPS coordinates: S 22°25.001' E015°51.156') in the dehydrated state in the dry winter season (June). The collected material was stored in the dry state at 20°C. Identification of the plant material was done by Jill Farrant (Moore et al., 2005a).

2.2.2 Polyphenol extraction from *Myrothamnus flabellifolia*

Polyphenols were extracted following the method by Makkar et al., 1993. Air dried leaves of *M. flabellifolia* were manually ground using a pestle and mortar to a fine powder in the presence of liquid nitrogen. The ground sample was passed through a 0.5 mm mesh sieve and weighed. Hexane (20 ml) was added to two centrifuge tubes each containing 1.5 g of the sieved sample material. The tubes were purged with nitrogen gas, covered and then sonicated for 30 minutes at room temperature. The sonicated mixture was centrifuged for 10 minutes at 10,000 x g. The pellet was re-extracted with hexane and then dried *in vacuo*. Aqueous acetone (70 % (v/v) acetone, 20 ml) was added to the pellet, which was purged with nitrogen and sonicated as before, and then centrifuged. Acetone extraction was performed twice and the resulting supernatant extracts from both tubes were pooled. Solvent extraction was performed three times by adding hexane to the acetone extract solution in a separating funnel. Polyphenols were collected from the bottom aqueous acetone layer. Acetone was removed from the polyphenol extract by

rotory evaporation under reduced pressure at 30 °C for two hours. The polyphenol extract was lyophilized and then stored at -20 °C.

2.2.3 Folin-Ciocalteau analysis of phenolics in crude and pure polyphenol extracts

Total phenolics in the extract were determined using the method of Makkar, 2003. Aliquots of gallic acid (0 to 5 µg/ml) were transferred to different test-tubes and the volume made up to 0.7 ml with distilled water. Folin-Ciocalteau reagent (1 M, 0.3 ml) was added followed by 1.0 ml sodium carbonate (20 % w/v), to give a final volume of 2.0 ml. The tubes were vortexed and incubated for 2 hours at 20 °C before measuring absorbance at 765 nm (Mozetic et al., 2006).

2.2.4 Polyphenol purification by Sephadex LH-20

The crude lyophilized polyphenol extract (62 mg) was dissolved in aqueous methanol (10 % , 4 ml) by sonication for 5 min, after which, the relatively small amounts of insoluble material was removed by centrifugation. The supernatant fraction was applied to a Sephadex LH-20 (Amersham Pharmacia Biotech AB SE-751 Uppsala Sweden) column (packed volume of 11 ml) equilibrated in water. Fractions were eluted with increasing concentrations of methanol in water (between 0 and 100 %). The absorbance at 280 nm of the fractions was determined to calculate the relative contribution to the original extract before samples were concentrated at 30 °C, under reduced pressure in a rotary evaporator, and subsequently lyophilized.

2.2.5 HPLC analysis of the crude and pure polyphenol extracts

High performance liquid chromatography (HPLC) analysis of the crude and purified polyphenols was performed using a Shimadzu LC-10 system (Japan) equipped with a Shimadzu SPD-M6A Photodiode array UV/VIS detector. Compounds were separated on a 250 mm x 4.6 mm, 5 µm particle size, Jones C18 column (USA) equilibrated using 0.1 % (v/v) trifluoroacetic acid (TFA) in water followed by a 0 – 100 % acetonitrile gradient in 0.1 TFA. The flow rate was 700 µl/min, at room temperature (22°C). Fractions eluted from Sephadex LH-20 column were analysed singly or in combination with other fractions. Fractions were compared to one another by co-injection (10 µl each) and the predominant peak was assumed to be 3,4,5 tri-o-galloylquinic acid (Moore et al., 2005b)

2.2.6 MALDI-TOF.MS analysis of the crude and pure polyphenol extracts

MALDI–TOF.MS analysis was performed according to the method of Moore et al., 2005. The sample was dissolved in 50 % acetonitrile and analysed using 10 mg dihydrobenzoic acid (DHB) matrix dissolved in 1 ml of 60 % acetonitrile and 0.1 % TFA. The MALDI mass spectrometer (Perseptive Biosystems DE – Pro) was used in the delayed extraction (DE) mode and positive ions were analyzed.

2.3 RESULTS AND DISCUSSION

2.3.1 Folin-Ciocalteau analysis of phenolics in crude and pure polyphenol extracts

Gallic acid solution was mixed with the Folin-Ciocalteau reagent, followed by sodium carbonate. After incubation for two hours at room temperature, the absorbance was measured at 765 nm. The results showed a direct relationship between the reduction of the Folin reagent and the concentration of gallic acid (Figure 2.1)

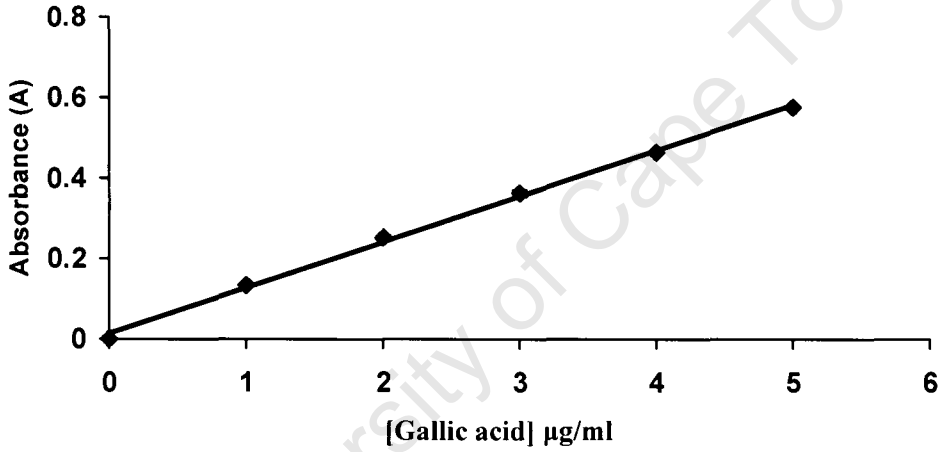

Figure 2.1: Standard curve for the Folin-Ciocalteau assay using gallic acid as a standard.

The absorbance was measured at 765 nm. The data represents the mean (±SD) of three replicate samples.

2.3.2 Polyphenol purification by Sephadex LH-20

The polyphenol extract from *M. flabellifolia* leaves was dissolved in aqueous methanol and fractionated using a Sephadex LH-20 column with increasing concentration of aqueous methanol. The elution was monitored by measuring the absorbance at 280 nm. The aim of this analysis was to isolate 3,4,5 tri-*O*-galloylquinic acid (TGQ), the major polyphenol from Namibian *M. flabellifolia* leaves (Moore et al. 2005). The chromatographic profile with five peaks (F_1, F_3-F_6) of 280 nm absorbing material is shown in Figure 2.2. No components were eluted using 10 % methanol (fractions in range F_2).

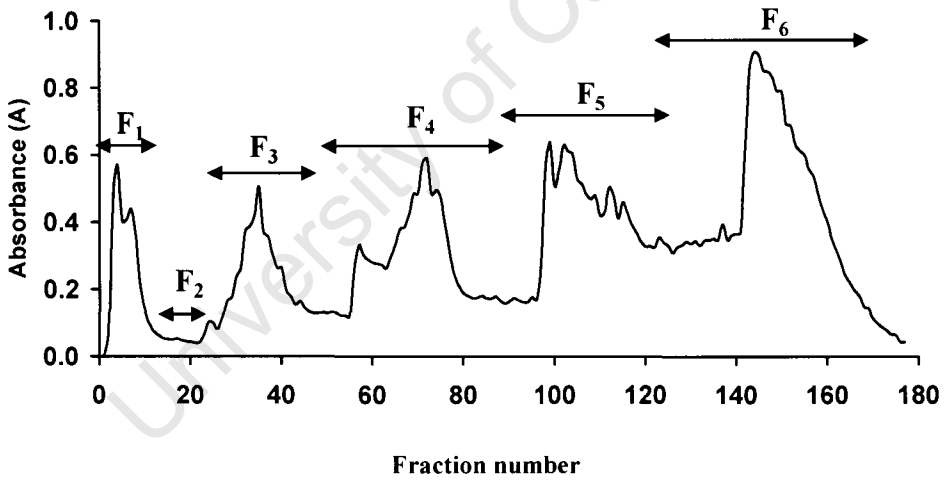

Figure 2.2 : The elution profile of polyphenols eluted from a Sephadex LH-20 column using water (F_1), 10% MeOH (F_2), 30% MeOH (F_3), 50% MeOH (F_4), 70% MeOH (F_5) and 100% MeOH (F_6). The absorbance was measured at 280 nm

Two independent experiments were performed and similar elution profiles were obtained in both cases. The amount of polyphenols in each fraction was estimated by measuring the absorbance of the pooled fractions at 280 nm (Table 2.1). This amount was expressed

as a percentage of the total absorbance of the original polyphenol sample. The largest amount of polyphenols was present in F_6 followed by F_5 and F_4. F_1 and F_3 registered the lowest amounts.

Table 2.1: An estimation of the percentage of polyphenols in each fraction eluted from Sephadex LH-20

Fraction	Amount of polyphenol (%)
F_1	11 ± 1.0
F_3	12 ± 0.5
F_4	18 ± 0.2
F_5	24 ± 6.0
F_6	38 ± 6.0

The water solubility of the lyophilized polyphenols from each fraction was tested. It was observed that F_1, F_3 and F_4 readily dissolved in water, whereas F_5 and F_6 were not readily soluble. It has been reported (Kantz and Singleton, 1990) that non-polymeric polyphenols are eluted from the Sephadex column matrix by 60 % methanol whereas polymeric polyphenols require more hydrophobic solvents. Fractions F_5 and F_6 probably contained several larger galloylquinic acid polymers (Moore et al., 2005), and may account for their insolubility and tighter binding to the column. This observation was supported by the fact all the fractions had ultraviolet absorption maxima near 280 nm which is characteristic of simple polyphenols i.e. gallic acid and gallic acid polymers (Sovak, 2001).

2.3.3 HPLC analysis of the crude and pure polyphenol extracts

Polyphenol fractions purified using Sephadex LH-20 chromatography were analysed using C18 reverse phase HPLC. Each fraction was screened for the presence of 3,4,5 tri-*O*-galloylquinic acid. The HPLC profiles for the crude and pure polyphenol fractions are shown in Figure 2.3. The HPLC profile for the crude extract showed 6 peaks, with one characteristic major peak. The first fraction (F_1) eluted from the Sephadex LH-20 contained at least 4 peaks with very small amount of 3,4,5 tri-*O*-galloylquinic acid.

The HPLC profile for fraction F_3 showed one large peak. It was observed that the retention time for the single peak in F_3 was similar to the retention time for the major peak of the crude extract profile. This was confirmed by co-injecting the two fractions onto the HPLC column. The profile showed an enhanced peak at the same retention time, suggesting that 3,4,5 tri-*O*-galloylquinic acid was eluted with 30 % methanol. The profile for polyphenols eluted with 50 % methanol (F_4) also showed a single major peak. This peak was confirmed by co-injection with F_3 to be 3,4,5 tri-*O*-galloylquinic acid, suggesting that 3,4,5 tri-*O*-galloylquinic acid was still bound to the column. The profile for 70 % methanol (F_5) showed four elution peaks. Co-injecting it with F_3, it became evident that 3,4,5 tri-*O*-galloylquinic acid was not present. As expected, 3,4,5 tri-*O*-galloylquinic acid was also not detected in the 100 % methanol eluted fraction (F6). Based on these results, it would appear that 3,4,5 tri-*O*-galloylquinic acid was optimally eluted with a methanol concentration in the 30 – 50 % range.

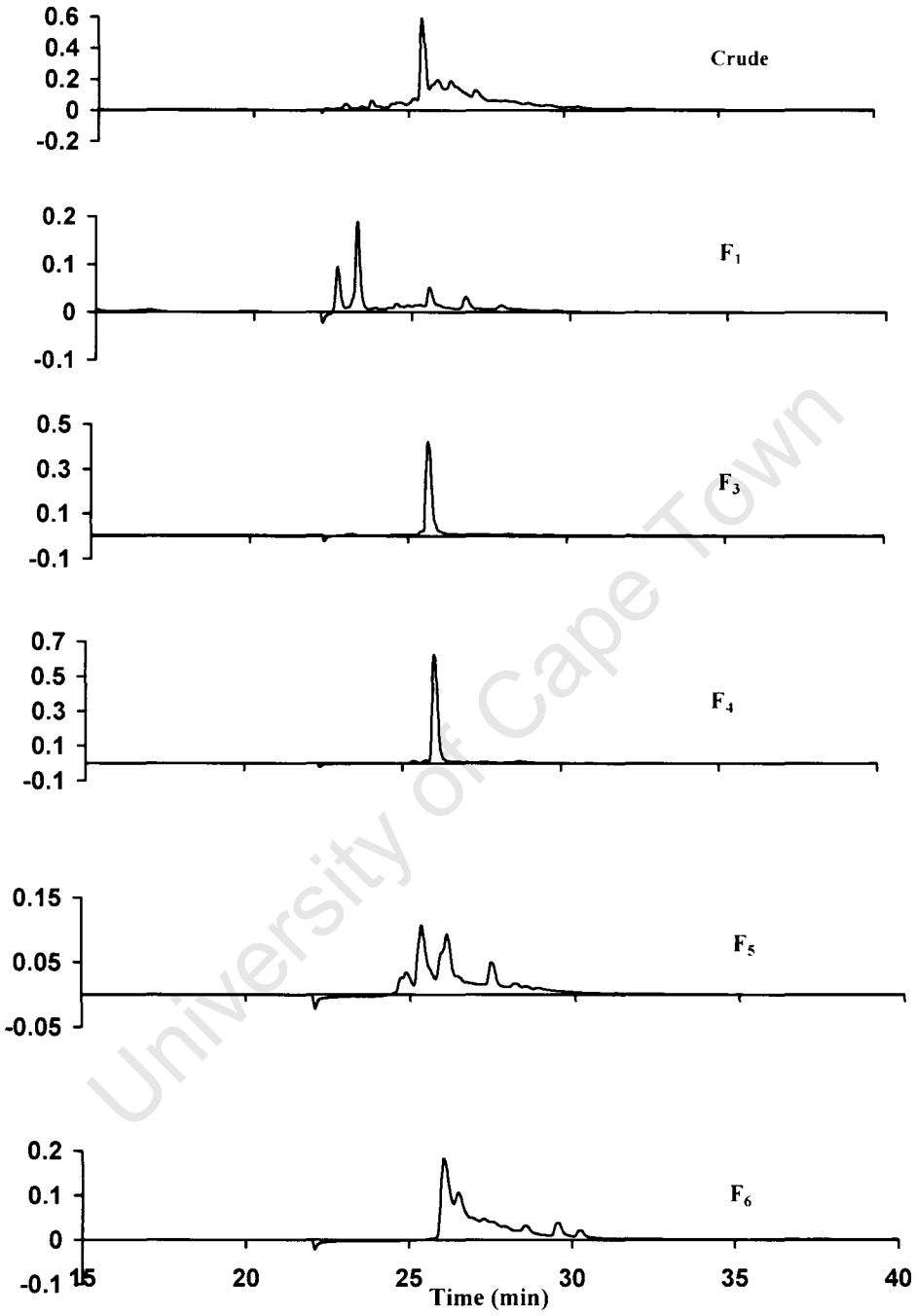

Figure 2.3: HPLC profile for crude and purified polyphenol fractions

The Y-axis represents the absorbance (mA) of polyphenols at 280 nm

2.3.4 MALDI-TOF.MS analysis of the crude and pure polyphenol extracts

The MALDI-TOF mass spectra for the crude and pure polyphenol extracts are shown in Figure 2.4. The peaks observed at m/z ratio below 600 were due to the dihydrobenzoic acid matrix. The spectrum of the crude extract showed several peaks with m/z ratios ranging from 600-1800. This range included two peaks "a" and "b" at m/z ratios of 671.34 and 687.34 respectively. The spectra for fractions purified by 30 % (F_3) and 50 % (F_4) methanol showed two major peaks "a" and "b" with m/z ratios similar to the two peaks "a" and "b" in the spectrum of the crude polyphenol extract. The molecular weight of a polyphenol fraction from *M. flabellifolia* leaves eluted with 30 or 50 % methanol from sephadex LH-20 has been reported to be 648 Da (Moore et al., 2005). No peak was, however, observed at m/z ratio of 648, characteristic of 3,4,5 tri-*O*-galloyquinic acid. It has been reported that the presence of Na^+ and K^+ ions during desorption and ionization results in the formation of $[M+Na]^+$ and $[M+K]^+$, where M represents the molecular weight of the parent molecule (Reed et al, 2005). The calculated m/z ratio of 3,4,5 tri-*O*-galloyquinic acid together with a sodium ion was 670.99 and the observed average ratio was 671.41. The calculated m/z ratio of 3,4,5 tri-*O*-galloyquinic acid together with a potassium ion was 687.10 whereas the observed average ratio was 687.39. It can therefore be concluded that the peaks observed at 671.41 and 687.39 were the Na^+ and K^+ adduct ions of 3,4,5 tri-*O*-galloyquinic acid molecule respectively. The spectra of the fractions eluted with 70 % (F_5) and 100% (F_6) methanol did not show any evidence for the presence of 3,4,5 tri-*O*-galloyquinic acid. The latter spectrum contained higher molecular weight compounds which have been reported to be formed by depside bonds

or oxidative addition of gallic acid moieties to 3,4,5 tri-*O*-galloylquinic acid (Moore et al., 2005)

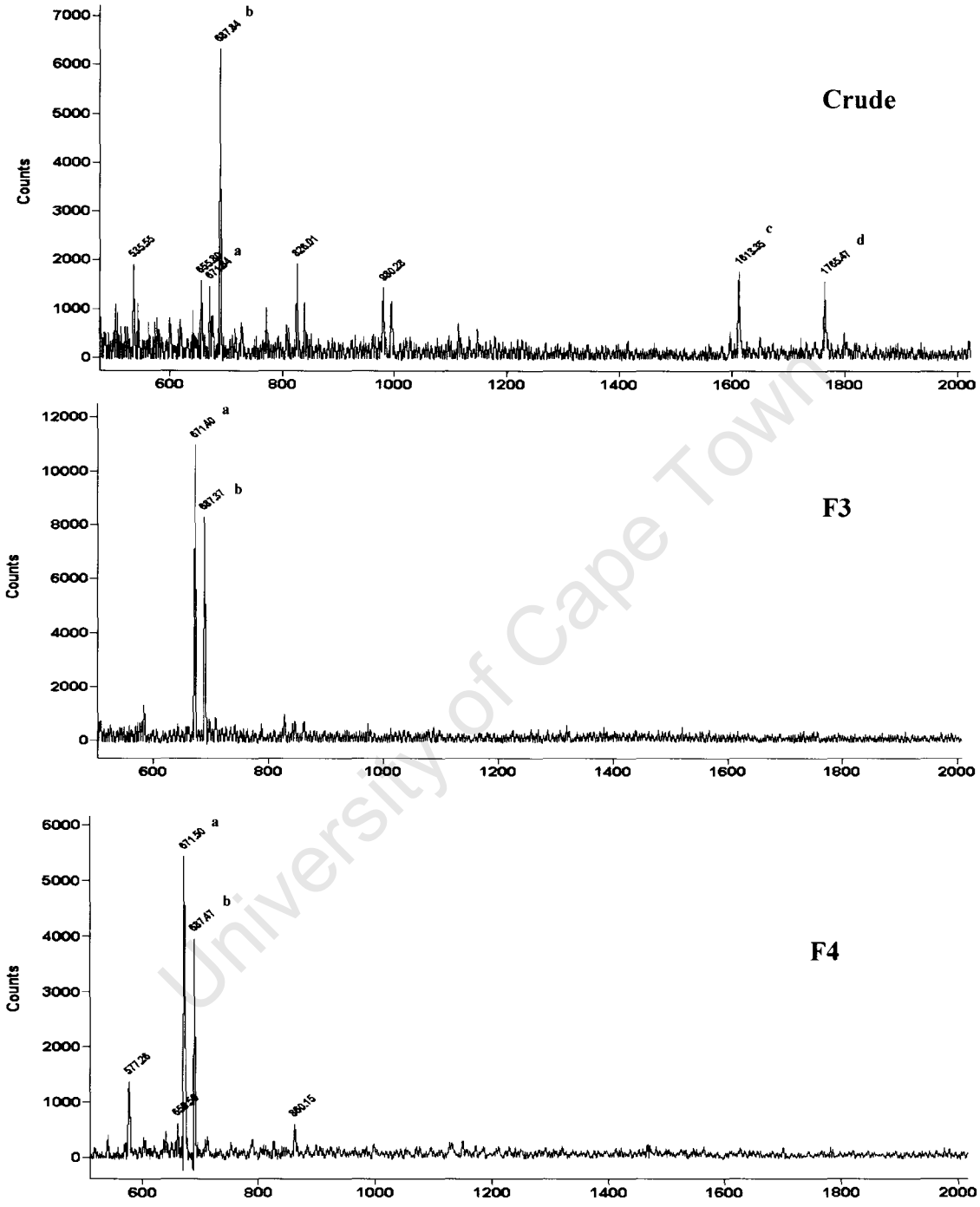

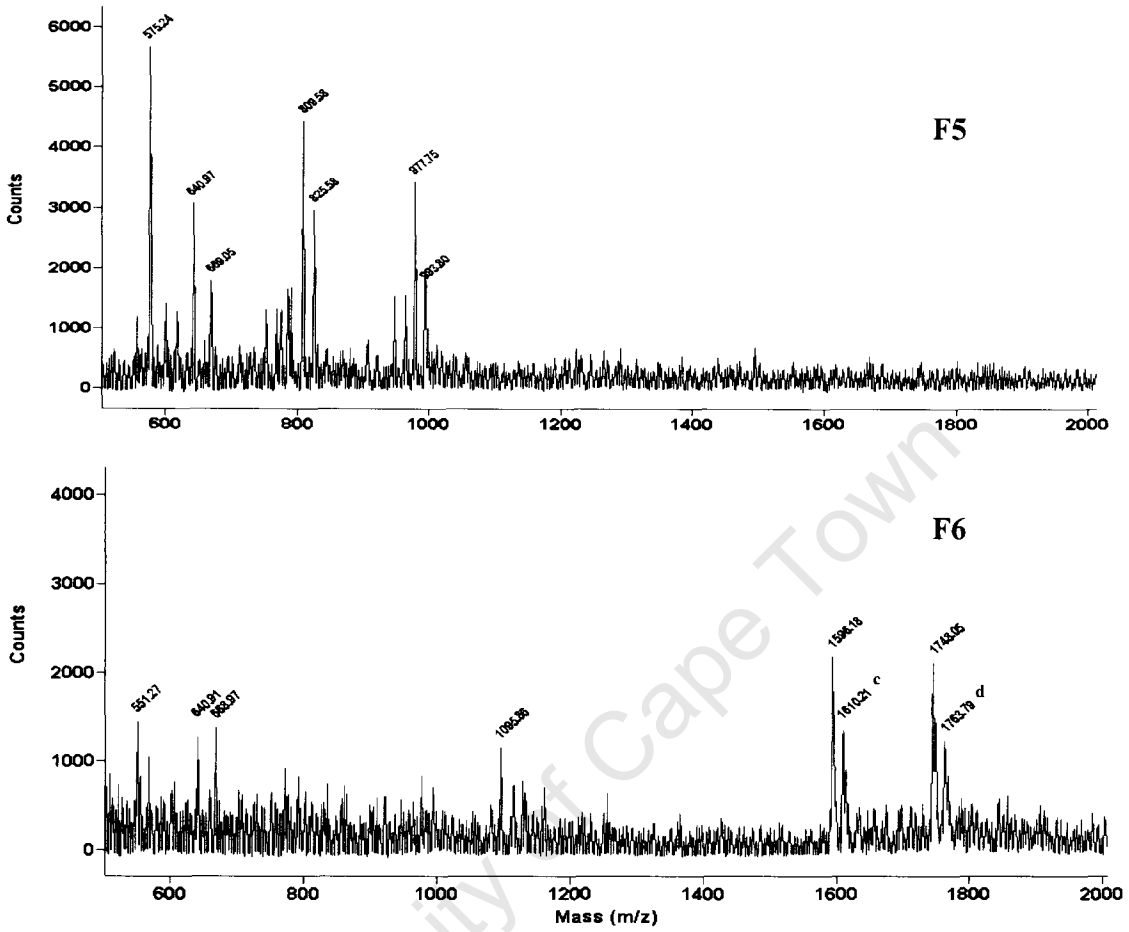

Figure 2.4: MALDI-TOF spectra of the crude polyphenol extract (crude) and fractions purified by Sephadex LH-20 column chromatography: F3-F6.

The peaks "a" and "b" were identified as $[TGQ + Na]^+$ and $[TGQ + K]^+$ respectively.

CHAPTER 3

ENZYMOLOGY OF REVERSE TRANSCRIPTASE

3.1 Introduction

DNA polymerases are divided into seven classes including reverse transcriptases (RTs) based on sequence homologies and crystal structures (Yang et al., 2004). RTs are known to have RNA/DNA-dependent polymerase and ribonuclease (RNase) H activities (Fisher et al., 2005). HIV-1 RT is one important example of a RT as it plays a crucial role in the life cycle of human immunodeficiency virus type 1 (HIV-1) (Goldschmidt et al., 2006). As such, it has been a major target of many antiviral drug therapies such as Nevirapine. As a non-nucleoside inhibitor, Nevirapine suffers from a rapid selection of resistant HIV strains. This resistance has generally been associated with Tyr 181 and Tyr 188 mutations within the NNRTIs binding pocket (Ren and Stammers, 2005). Thus the need for new inhibitors for HIV-1 RT can not be over-emphasized. Moloney murine leukemia virus reverse transcriptase (M-MLV RT) is another RT, which is extensively used in molecular biology applications such as cDNA synthesis on account of its relatively low cost.

Assays for RT activities are widely based on the incorporation of radio-labeled deoxynucleotides into the primer template complex (Nishizawa et al., 1989). In this study, a non radioactive assay for RT activity was developed. The assay was based on ethidium bromide fluorescence and it was successfully optimized using M-MLV RT. Finally, the inhibition of HIV-1 and M-MLV RTs by crude and pure polyphenol extracts from *M. flabellifolia* was tested.

3.2 Materials and Methods

3.2.1 Chemicals and Reagents

Calf thymus DNA was purchased from Sigma. Poly(rA) template (approximately 1000 bases) was a donation from Ribotech. An oligo$(dT)_{25}$ primer was purchased from UCT MCB DNA Services. The reverse transcriptase enzymes M-MLV-RT and HIV RT were purchased from Promega and Ambion respectively. The ultra-pure lithium salts of dTTP, dATP, dCTP, and dGTP were products of Bioline. dAMP, ATP, and thymidine were purchased from Sigma. Thymine was purchased from Merck. Tris-HCl and ethidium bromide were from Research Organics and Merck respectively. Sodium pyrophosphate was purchased from Riedel-De Hahn.

3.2.2 DNA Quantification by Fluorometry

Calf thymus DNA (ctDNA) was chosen as a standard for DNA quantification. ctDNA was dissolved in double distilled water and its final concentration was determined by spectrophotometry (NanoDrop ND-1000 Spectrophotometer). ctDNA was diluted in Tris-HCl buffer (40 mM Tris, 100 mM NaCl, pH 7.2) to give a concentration range of 0 to 8 µg/ml. Ethidium bromide was added to a final concentration of 2.5 µg/ml. Tris-HCl buffer was added to bring the final volume to 1.0 ml. Tris-HCl buffer and ethidium bromide were prepared using double distilled and sterilized water. Fluorescence was measured using an Aminco SPF 500 fluorometer. The excitation wavelength was 545 nm with a 5 nm bandpass, and the emission wavelength was 605 nm with a 10 nm bandpass. The effect of polyphenols on the fluorescence of the

ctDNA-ethidium bromide complex was performed in the presence of 34 μM final polyphenol (3,4,5 tri-*O*-galloylquinic acid) concentration.

3.2.3 Poly (rA) and oligo $(dT)_{25}$ titration

Poly (rA) template solution was prepared by dissolving the polymer in RNase free water and the concentration was determined spectrophotometricaly. The poly (rA) solution was diluted to a working concentration of 1.00 μg/μl. Poly (rA) (2.5 μg) was mixed with various amounts of oligo$(dT)_{25}$ primer up to 5 μg. The final volume of the solution of poly (rA) and oligo $(dT)_{25}$ mixture was made to 50 μl with RNase free water. Poly(rA) was omitted from the control reaction. The mixture was incubated at 65 °C for 5 minutes, chilled on ice for at least 1 minute and then incubated at room temperature for 15 minutes. Tris-HCl buffer (945.0 μl, pH 7.2) and ethidium bromide (5 μl, 0.5 mg/ml) was added to the mixture to bring the final volume to 1.0 ml. Ethidium bromide fluorescence was measured as before.

3.2.4 Assay for M-MLV and HIV-1 RT activity

First strand cDNA synthesis using M-MLV and HIV-1 RT was performed according to their respective manufacturer's protocol with some changes. Poly (rA) template (12.5 μg) and oligo $(dT)_{25}$ primer (0.25 μg) were mixed to give a total volume of 25 μl. The mixture was centrifuged briefly and then incubated at 65 °C for 5 minutes. The mixture was then chilled on ice for at least 1 minute and allowed to stand at room temperature for 15 minutes. Reagents for M-MLV RT assay were added to the Poly (rA).oligo $(dT)_{25}$ mixture in the following order : M-MLV-RT buffer (5X, 25 μl),

dTTP (up to 4 mM final concentration), and RNase free water. The mixture was centrifuged briefly to bring the contents to the bottom of the tube. M-MLV RT enzyme (170 Units, 0.071 μM) was added to the mixture to give 100.0 μl final assay volume, mixed by gently tapping the bottom of the tube, briefly centrifuged as before and then immediately incubated at 37 °C. Reagents for HIV-1 RT assay were added to the poly (rA).oligo $(dT)_{25}$ mixture as follows: HIV-1 RT buffer (10X, 16.7 μl), dTTP (0 to 2 mM) and RNAse free water to make the final volume to 25 μl. The mixture was treated as per the M-MLV RT assay before addition of HIV-1 RT enzyme (20 U, 0.17 μM). The mixture was incubated at 42 °C. Aliquots (20 μl) were taken at every 5 minute time interval and immediately added to Tris-HCl buffer (975 μl pH 7.2,) containing ethidium bromide (2.5 μg/ml) to a final volume of 1.0 ml. Ethidium bromide fluorescence was measured as before.

3.2.5 Effect of potential inhibitors on M-MLV RT activity

The assay for M-MLV RT activity was performed in the presence of 1.0 mM dTTP and either dATP, dCTP, dGTP, dAMP, ATP, thymidine, thymine, pyrophosphate or phosphate. All additional compounds were added to a final concentration of 1.0 mM.

3.2.6 Effect of polyphenols on M-MLV and HIV-1 RT activity

The effect of crude and purified polyphenols (F_1, F_2 –F_6) on enzyme activity was initially performed using M-MLV RT in the presence of 1.2 μg/ml final polyphenol concentration. The dTTP and Mg^{2+} concentrations were fixed at 1.0 and 3.75 mM respectively. Polyphenol fractions which exhibited 100 % M-MLV RT inhibition were

diluted and re-assayed. The most effective polyphenol fraction was further analysed to establish the 50 % inhibitory concentration (IC_{50}) values for both M-MLV and HIV-1 RTs. Polyphenols were omitted from control reactions. The effect of Nevirapine on M-MLV and HIV-1 RT was performed using Nevirapine concentrations of up to 1.0 mM and 1.0 μM for M-MLV and HIV-1 RT respectively.

3.2.7 Mode of 3,4,5 tri-*O*-galloylquinic acid inhibition of M-MLV and HIV-1 RT activity

An enzyme activity assay to determine the nature of the polyphenol inhibition of M-MLV and HIV-1 RT was carried out in the presence of 0.5 μM and 34 μM 3,4,5 tri-*O*-galloylquinic acid respectively. The concentration of Mg^{2+} ions was held constant at 3.75 mM and dTTP concentrations up to 1.0 mM were used for M-MLV RT, whereas 5.0 mM Mg^{2+} and dTTP concentrations up to 0.25 mM were used for HIV-1 RT.

3.2.8 Reversibility of 3,4,5 tri-*O*-galloylquinic acid binding to M-MLV and HIV-1 RT

To determine how tightly polyphenols were bound to the M-MLV RT enzyme, soluble PVP and BSA were added to the cDNA synthesis assay, either alone or in combination with 3,4,5 tri-*O*-galloylquinic acid. The final concentration of PVP and BSA in the assay mixture was 0.03 mg/ml, resulting in the molar ratio of PVP to M-MLV RT and BSA to M-MLV RT of 11:1 and 63:1 respectively. The final 3,4,5 tri-*O*-galloylquinic acid concentration used was 2.4 μM. The assay was performed as follows: (i) PVP or BSA was added in the absence of 3,4,5 tri-*O*-galloylquinic acid followed by M-MLV RT and

then immediately incubated at 37 °C. (ii) The enzyme was initially mixed with 3,4,5 tri-*O*-galloylquinic acid, briefly mixed by tapping the tube at the bottom and centrifuged to mix the contents and then allowed to stand in ice for 5 minutes. PVP or BSA was then added and the mixture allowed to stand on ice for another 5 minutes before performing the enzyme assay. (iii) PVP or BSA was initially added to the assay mixture containing 3,4,5 tri-*O*-galloylquinic acid, mixed thoroughly and allowed to stand on ice for 5 minutes before adding M-MLV RT.

The mode of 3,4,5 tri-*O*-galloylquinic acid inhibition of HIV-1 RT was performed in the presence of 100 μM 3,4,5 tri-*O*-galloylquinic acid and 11.0 μM BSA. The molar ratio of BSA to HIV-1 RT was 63:1. The enzyme activity assay was initially performed in the presence of 3,4,5 tri-*O*-galloylquinic acid and BSA alone. Secondly, The HIV-1 RT enzyme was mixed with 3,4,5 tri-*O*-galloylquinic acid and allowed to stand for 5 minutes on ice before BSA addition. Finally, BSA was mixed with 3,4,5 tri-*O*-galloylquinic acid, allowed to stand for 5 minutes on ice before HIV-1 RT enzyme addition. cDNA synthesis by HIV-1 RT was performed at 42°C. Ethidium bromide fluorescence was measured to follow the progress of cDNA synthesis as before.

3.3 RESULTS AND DISCUSSION

3.3.1 DNA Quantification

The RT assay was designed to synthesise cDNA from a poly (rA) template using an oligo$(dT)_{25}$ primer together with dTTP. The initial objective was to set up a method to determine low concentrations of dsDNA in solution. The method used was based on ethidium bromide fluorescence and assumes that the binding of ethidium bromide to dsDNA and its subsequent fluorescence is equivalent to binding to cDNA. Although the fluorescence of free ethidium bromide in solution is very low, the fluorescence is greatly enhanced when it intercalates into the DNA double helix. This enhanced fluorescence is thought to arise from shielding of the ethidium bromide from the quenching effect of the surrounding water molecules (Garbett et al., 2004). Calf thymus DNA was chosen as the standard to determine the DNA concentration in solution. The results showed that the ethidium bromide fluorescence was directly proportional to the DNA concentration in the range of 0 - 8 µg/ml. (Figure 3.1). The R^2 value of 0.997 demonstrated a linear response for ethidium bromide fluorescence over this concentration range. The limit of sensitivity using this method was approximately 0.1 µg/ml. In comparison, the limit of detection using a UV spectrophotometer is approximately 5 µg/ml assuming that a 1 mg/ml of DNA solution has an A260 nm = 20. Polyphenols through their planar aromatic groups have the potential to either enhance or quench the fluorescence of the ethidium bromide-DNA complex in solution. The effect of these polyphenols on the fluorescence of ctDNA-ethidium bromide complex was investigated in the presence of 34 µM final

3,4,5 tri-*O*-galloylquinic acid concentration. The results showed no significant change in the fluorescence of the ctDNA-ethidium bromide complex in the presence or absence of polyphenols. Furthermore fluorescence measurements for enzyme assays (section 3.2.4 - 3.2.6) were performed after a 50 fold dilution of the assay mixture (including the polyphenol concentration) while ethidium bromide concentration remained constant at 2.5 µg/ml.

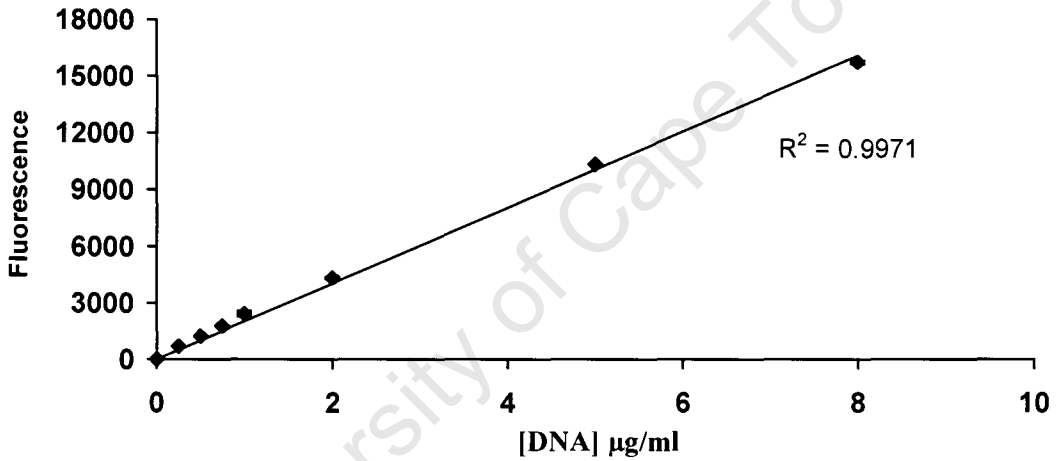

Figure 3.1: Calibration curve for the determination of DNA in solution.

Ethidium bromide in water was added to a final concentration of 0.025mg/ml to various concentrations of calf thymus DNA in Tris-HCl pH 7.2. The fluorescence was determined at 605 nm (excitation 545nm). The data represent the mean (± SD) of three replicate samples. Error bars not visible are within the symbols.

3.3.2 Poly (rA) and oligo(dT)$_{25}$ titration

The RT assay was based on the elongation of an oligo.dT primer of length 25 nucleotides (oligo (dT)$_{25}$) bound to a poly (rA) template of length approximately 1000 nucleotides. In order to determine whether binding of the primer to the template occurred and whether this was saturable at the theoretical maximum, increasing amounts of primer were added to a fixed amount of template. The amount of double-stranded nucleic acid formed would be determined from the ethidium bromide fluorescence. After heating at 65°C for 5 mins to achieve complete denaturation, the samples were rapidly cooled on ice for 5 minutes. Ethidium bromide was then added to a final concentration of 25 µg/ml and the fluorescence determined as described. The results showed that ethidium bromide fluorescence increased linearly up to when 2.5 µg oligo (dT)$_{25}$ was added per 2.5 µg poly (rA), after which it remained constant. Thus an equivalent amount of oligo (dT)$_{25}$ was required to form the maximum amount of double stranded nucleic acid, showing that the entire length of the poly (rA) template interacted with the primer when sufficient primer was present. No change in the ethidium bromide fluorescence was observed when the poly (rA) template was omitted.

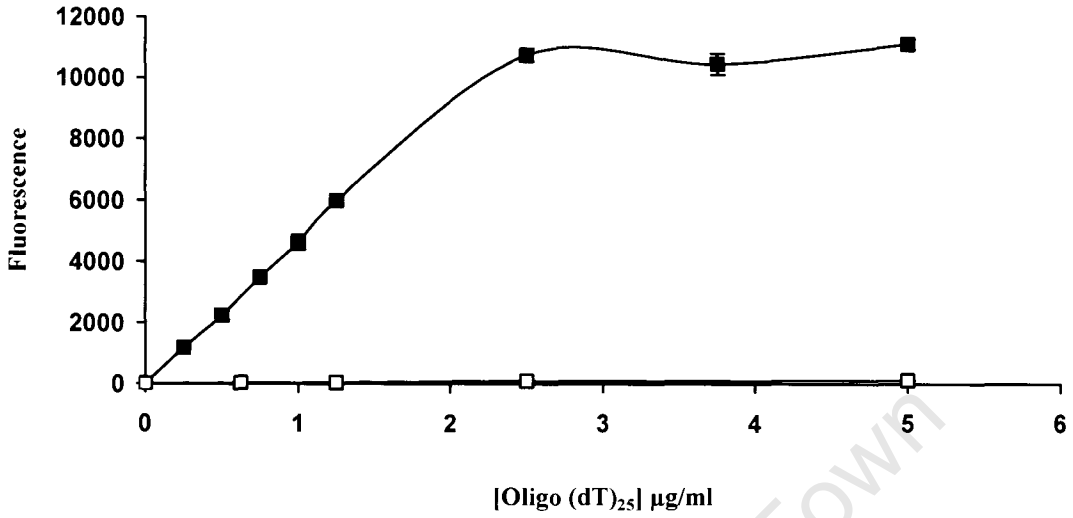

Figure 3.2: Ethidium bromide fluorescence as a function of the concentration of oligo $(dT)_{25}$.

Oligo $(dT)_{25}$ was added to 2.5µg/ml poly (rA) (■) to a final concentration up to 5µg/ml. Ethidium bromide was then added to 25 µg/ml and the fluorescence was determined as before. Poly (rA) was omitted from the control titration. (□). 2.5 µg of oligo $(dT)_{25}$ added corresponded to a theoretical 5.0 µg cDNA formed. The data represent the mean (± SD) of three replicate samples.

The response of ethidium bromide binding to DNA (Figure 3.1) was compared with its binding in the linear region to the oligo $(dT)_{25}$.poly (rA) duplex (Figure 3.2). These responses were found to be 2012 ± 7 and 2222 ± 54 U/µg/ml respectively suggesting that calf thymus DNA was a reasonable standard against which the cDNA could be quantitated.

3.4 Enzymology of M-MLV Reverse Transcriptase

The RT assay was designed to extend the oligo $(dT)_{25}$ primer bound to the poly (rA) template using dTTP in the presence of 3.75 mM Mg^{2+}. A ratio of 1: 50 oligo $(dT)_{25}$:poly (rA) (g/g) was used together with dTTP in the concentration range 0.0 to 4.0 mM. If the reaction were allowed to go to completion, 25.0 µg of double stranded cDNA would be formed. Samples were removed from the assay mixture at selected time points, ethidium bromide was added to 25 µg/ml final concentration and the fluorescence determined. The linear portion of the reaction profile yielded V_o, the initial velocity of the reaction. Typical reaction profiles are shown in Figure 3.3. The concentration of cDNA synthesized was calculated from the ethidium bromide fluorescence.

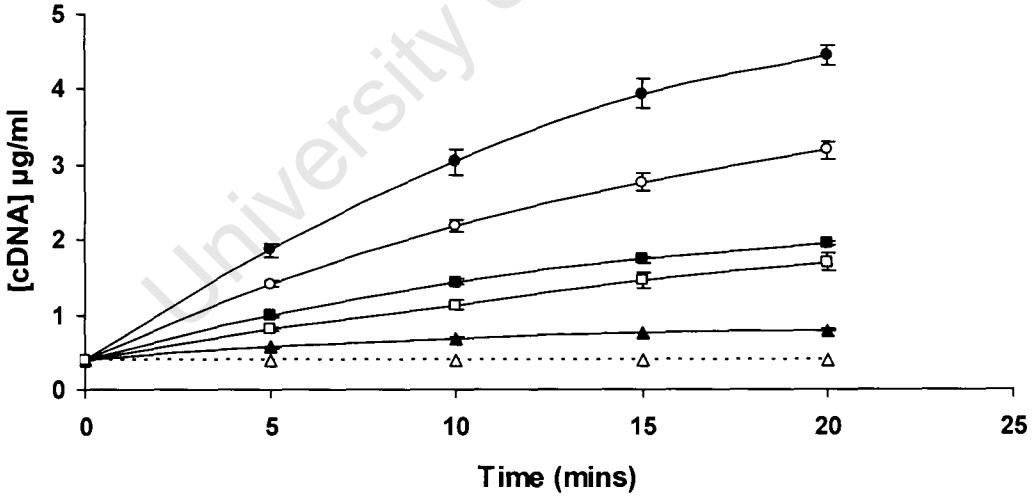

Figure 3.3: cDNA synthesis using selected dTTP concentrations as a function of time.

The dTTP concentrations (mM) used were: 0.00 (Δ), 0.0625 (▲), 0.25 (■), 0.50 (○), 1.0 (●), 3.0 (□)

A plot of the initial velocity (V_0) against the substrate concentration showed that an increased reaction rate occurred as a function of the dTTP concentration. This rate reached a maximum at 1.0 mM dTTP (Figure 3.4). Further addition of dTTP resulted in a marked decrease in the rate of cDNA synthesis, which was virtually zero in the presence of 4.0 mM dTTP. This behaviour, referred to as substrate inhibition, where the rate of catalysis increases with an increased substrate concentration to a maximum velocity after which the rate decreases, has been reported as a common deviation from normal Michaelis-Menten kinetics (Kuhl, 1994).

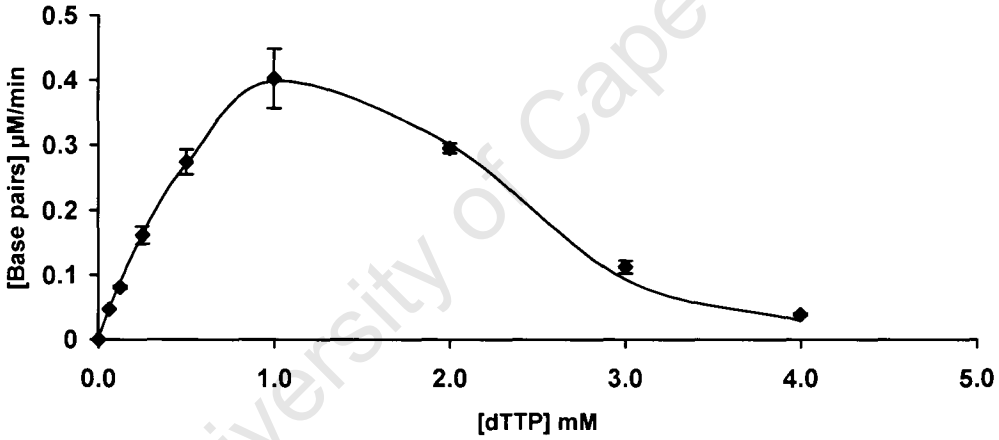

Figure 3.4: Initial rate (Vo) for the formation of cDNA as a function of the dTTP concentration.

The assay was carried out in the presence of 3.75mM $MgCl_2$.

Kinetic data implicating substrate inhibition needs to be interpreted with care. Competitive substrate inhibition has been implicated in causing substrate inhibition, but its effect becomes negligible when initial rates are used (Verhamme et al., 1988). The presence of contaminating noncompetitive inhibitors in the substrate has also been reported to give rise to apparent substrate inhibition (Verhamme et al., 1988). However,

this was unlikely as the dTTP was at least 99 % pure. Another factor that can cause substrate inhibition is a substrate co-factor (Dixon & Webb, 1979). M-MLV reverse transcriptase requires Mg^{2+} for its catalytic activity and this would be considered to be a co-factor. Since high dTTP concentrations would bind to the Mg^{2+} present in the assay mixture (Oelschlaeger et al., 2007), it is possible that the substrate inhibition observed at high substrate concentration was caused by insufficient free Mg^{2+} in the assay mixture. To investigate if this was indeed the case, the assay was repeated in the presence of 7.5 mM Mg^{2+}. The results showed that there was no difference in the reaction rate up to 1 mM dTTP when compared with the reaction in the presence of 3.75 mM Mg^{2+} (Figure 3.5). However, the maximum rate observed now occurred at 2 mM dTTP, after which the rate was found to decrease. This decrease was markedly less than that observed in the presence of 3.75 mM Mg^{2+}. When the molar ratio Mg^{2+}: dTTP was 1:1, the M-MLV RT activities observed were equivalent, strongly suggesting that inhibition of enzyme activity at high substrate concentration was probably due to interaction between the Mg^{2+} and the dTTP.

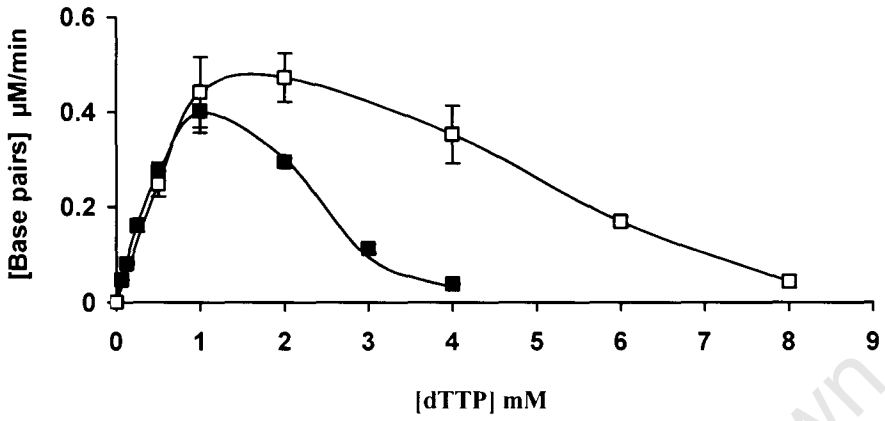

Figure 3.5: Initial rate (Vo) for the formation of cDNA as a function of the dTTP concentration.

The assay was carried out in the presence of either 3.75 mM $MgCl_2$ (■) or 7.5 mM $MgCl_2$ (□). The data represent the mean (± SD) of two replicate samples.

3.4.1 Kinetic parameters for M-MLV RT activity

Kinetic parameters for an enzyme that exhibits inhibition at high substrate concentrations can be estimated by ignoring the contribution of higher substrate concentrations. The V_{max} and K_m are then estimated from the normal Michaelis-Menten kinetics using a double-reciprocal plot (Figure 3.6). V_{max} was found to be 0.8 ± 0.2 µM (bp)/min and K_m was found to be 1.06 ± 0.22 mM irrespective of whether the Mg^{2+} concentration was 3.75 or 7.5 mM. Addition of the kinetic data observed at high substrate concentrations in the presence of 3.75 mM Mg^{2+} resulted in a plot that curved upwards at high substrate concentrations.

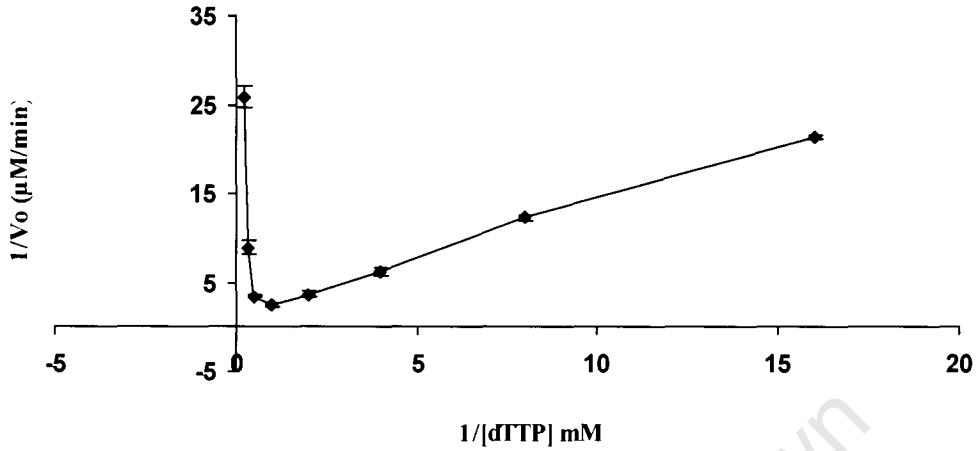

Figure 3.6: Double-reciprocal plot of the initial velocity of dTTP incorporation into poly (rA) : oligo (dT_{25}) by M-MLV RT as a function of the dTTP concentration.

3.4.2 Effect of potential competitive inhibitors on M-MLV RT activity

A number of nucleotide triphosphates and similar molecules were investigated as to whether these inhibited the M-MLV RT reaction. The compounds tested were dGTP, dCTP, dATP, ATP, dAMP, ADP, thymidine, thymine, pyrophosphate and phosphate. The Mg^{2+} and dTTP concentrations were fixed at 3.75 and 1.0 mM respectively and the compounds tested were present at a final concentration of 1.0 mM. The inhibition of M-MLV RT activity of these compounds was compared to the inhibition observed with 2 mM dTTP.

The results showed that all nucleotide triphosphates (dGTP, dCTP, dATP and ATP) inhibited M-MLV RT activity significantly, and were comparable to the inhibition observed in the presence of 2.0 mM dTTP (Table 3.1). Pyrophosphate also showed a significant but lesser inhibition by comparison with the nucleotide triphosphates. The other compounds tested did not show any significant inhibition. No difference was observed if the sugar moiety of the nucleotide was ribose or deoxyribose. These data

showed that the presence of a triphosphate on the nucleotide is crucial. Whereas the triphosphate inhibition observed could be due to the binding of Mg^{2+} ions, the pyrophosphate inhibition observed might result from two distinct causes. Firstly, pyrophosphate might bind to the positions where the β and γ phosphates bind thereby competing with nucleotide triphosphate binding, and secondly pyrophosphate is a product of the RT reaction. Thus increased pyrophosphate concentrations would favour the reverse reaction and reduce the forward enzyme activity. It was considered that the observed inhibition was not due to Mg^{2+} binding, since nucleotide diphosphates would bind Mg^{2+} equivalently to pyrophosphate.

Table 3.1: M-MLV RT activity inhibition by potential competitive inhibitors.

1 mM of each test compound was mixed with 1mM dTTP and then assayed for enzyme activity. The data were compared with the activity observed in the presence of 2.0 mM dTTP which resulted in 35 ± 3 % inhibition. The data represent the mean (± SD) of three replicate samples.

Compound	Inhibition (%)
Deoxynucleotides	
dTTP	35 ± 3
dGTP	39 ± 3
dCTP	41 ± 6.
dATP	43 ± 4
dAMP	7 ± 5
Ribonucleotides	
ATP	38 ± 0.3
ADP	7 ± 8
Bases	
Thymine	9 ± 7
Deoxyribonucleoside	
Thymidine	10 ± 4
Other compounds	
Sodium pyrophosphate	23 ± 4
Phosphate	0

3.4.3 Effect of polyphenols on M-MLV RT activity

Preliminary data showed that crude polyphenol extracts of *M. flabellifolia* leaves inhibited M-MLV RT activity *in vitro*. The crude extract was separated into various fractions using Sephadex LH-20 chromatography which were analysed by HPLC and MALDI-TOF mass spectrometry. Only the main constituent in fractions F_3 and F_4 was identified and this was found to be 3,4,5 tri-O-galloylquinic acid. The assay for M-MLV RT activity was, however, performed on all HPLC fractions although the main constituents were unknown. The final concentration of each polyphenol fraction used to test for the inhibitory activity of M-MLV RT was 1.2 µg/ml. At this concentration, the crude extract and fractions F1, F5 and F6 inhibited M-MLV RT by up to 84 % (Table 3.2). In contrast, complete inhibition was found for fractions F_3 and F_4. These fractions were diluted 4-fold and re-assayed. At a concentration of 0.3 µg/ml, these fractions exhibited identical inhibitory activity of approximately 35 %.

Table 3.2: Effect of crude and pure polyphenol fractions on M-MLV RT activity.

The data represent the mean (± SD) of three replicate samples. Fractions F_3 and F_4 were diluted and then re-assayed at a final concentration of 0.3 µg/ml.

	Inhibition (%)	
Polyphenol fraction	**1.2 µg/ml**	**0.3 µg/ml**
Crude extract	54 ± 10	
F_1	34 ± 8	
F_3	98 ± 0.2	31 ± 5
F_4	98 ± 0.3	41 ± 8
F_5	33 ± 2	
F_6	84 ± 2	

All further work on polyphenol-mediated RT inhibition was performed using fraction F_3, pure 3,4,5 tri-*O*-galloylquinic acid. The concentration of 3,4,5 tri-*O*-galloylquinic acid required for 50 % inhibition of M-MLV RT (IC_{50}) was determined by adding various concentrations up to 0.9 µM of 3,4,5 tri-*O*-galloylquinic acid to the enzyme assay. The results showed an exponential response of M-MLV RT inhibition in this concentration range (Figure 3.7) and the IC_{50} was estimated to be 0.5 ± 0.004 µM.

Since polyphenols are known to chelate divalent metal ions, it is possible that the observed inhibition could be due to the polyphenol binding of Mg^{2+}. This however was very unlikely since Mg^{2+} ions were present in a 1000 fold excess over the polyphenol concentration.

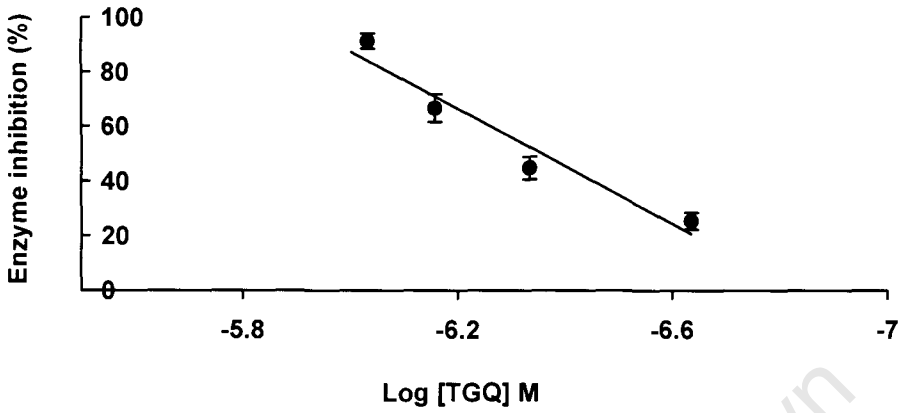

Figure 3.7: Inhibition of M-MLV RT activity as a function of the log (3,4,5 tri-*O*-galloylquinic acid) concentration.

The data represent the mean (± SD) of three replicate samples.

3.4.4 Mode of M-MLV RT inhibition by 3,4,5 tri-*O*-galloylquinic acid

Having established that 3,4,5 tri-*O*-galloylquinic acid inhibited M-MLV RT activity, the mode of this inhibition was investigated. The concentrations of 3,4,5 tri-*O*-galloylquinic acid and Mg^{2+} were fixed at 0.5 µM and 3.75 mM respectively. A Lineweaver-Burke plot of the data showed non-competitive inhibition by 3,4,5 tri-*O*-galloylquinic acid (Figure 3.8).

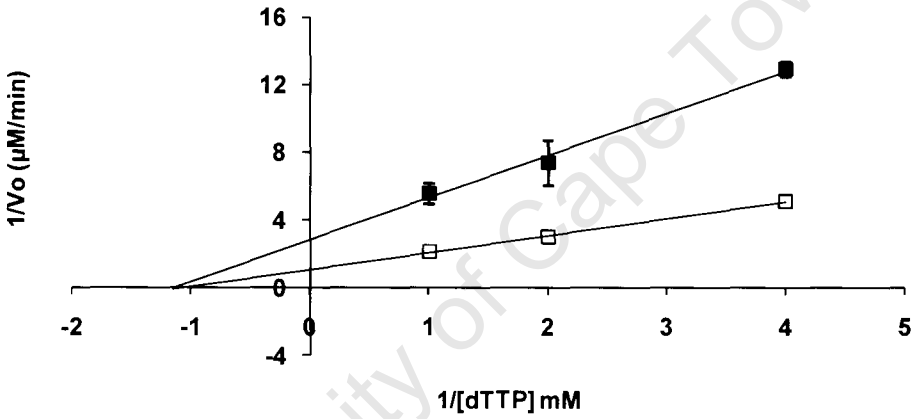

Figure 3.8: A Lineweaver-Burk plot of dTTP incorporation into poly (rA).oligo(dT_{25}) by M-MLV RT as a function of dTTP concentration in the presence (■) and absence (□) of 3,4,5 tri-*O*-galloylquinic acid.

The data represent the mean (±SD) of three replicate samples

The apparent change in maximum velocity (V_{max}^{app}) in the presence of 3,4,5 tri-*O*-galloylquinic acid is represented by the following equation (Garrett and Grisham, 2005):

$$V_{max}^{app} = \frac{Vmax}{(1 + [TGQ]/K_i)}$$

This equation is useful for estimating the inhibition constant (K_i) since V_{max} and V'_{max} can be deduced directly from the Lineweaver-Burke plot. The kinetic parameters are summarized in Table 3.3. The inhibition constant K_i represents the IC_{50} for a given compound. The value was very similar to the previous estimate of the IC_{50} (Figure 3.7). The K_m and V_{max} values of the uninhibited enzyme were very similar to those obtained previously (Figure 6), even though different batches of the enzyme were used

Table 3.3: Kinetic parameters for dTTP incorporation into poly (rA):oligo(dT)$_{25}$ complex using M-MLV RT, in the presence and absence of 3,4,5 tri-O-galloylquinic acid

Reaction velocity units represent the concentration of base pairs incorporated per minute

Parameter		No TGQ added	TGQ added
V_{max}	(μM/min)	0.95 ± 0.03	
V'_{max}	(μM/min)		0.36 ± 0.03
K_m	(mM)	0.90 ± 0.15	
K'_m	(mM)		0.90 ± 0.15
K_i	(μM)		0.31 ± 0.05

Non-competitive inhibition is exhibited by compounds with structures different from the substrates, in this case the nucleotide triphosphates (NTP's). The structure of 3,4,5 tri-*O*-galloylquinic acid (Figure 1.7) is clearly very different to the

structure of the NTP's. Non-competitive inhibitors bind to the enzyme at a site distinct from the active site, resulting in the enzyme complexes shown below:

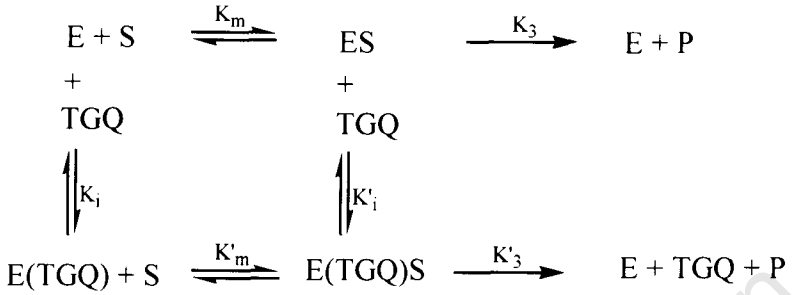

The scheme shows that the 3,4,5 tri-*O*-galloylquinic acid binds to both the free enzyme (E) and the enzyme substrate complex (ES). In non-competitive inhibition, the affinity of the enzyme for the substrate is unaffected by the presence of the inhibitor and vice versa, such that $K_i = K'_i$ (Whiteley, 2000).

3.4.5 Reversibility of 3,4,5 tri-*O*-galloylquinic acid binding to M-MLV RT

The binding of inhibitors to enzymes can either be reversible or irreversible. Reversible binding involves dissociation (at different rates) of the enzyme-inhibitor complex whereas no dissociation takes place during irreversible inhibition. To determine the reversibility of 3,4,5 tri-*O*-galloylquinic acid binding to M-MLV RT, an enzyme activity assay was performed in the presence of 3,4,5 tri-*O*-galloylquinic acid together with either PVP or BSA, which were used as a polyphenol binding agent and a competing protein respectively. The Mg^{2+} concentration was fixed at 3.75 mM. The results showed that the M-MLV RT activity in the presence of PVP and BSA alone was similar to that in their absence (Figure 3.9), showing that PVP and BSA did not inhibit M-MLV RT activity. The activity of the enzyme in the presence of 0.9 μM of

3,4,5 tri-*O*-galloylquinic acid was approximately 7 %. PVP or BSA addition subsequent to 3,4,5 tri-*O*-galloylquinic acid addition did not restore the activity of the enzyme, and in each case the activity was similar to that in the presence of 3,4,5 tri-*O*-galloylquinic acid alone. Since PVP was added at a molar ratio of PVP : M-MLV RT of 106:1 and BSA at a molar ratio of BSA:M-MLV RT of 63:1, it was apparent that 3,4,5 tri-*O*-galloylquinic acid was tightly or irreversibly bound to the enzyme. Addition of the M-MLV RT to 3,4,5 tri-*O*-galloylquinic acid in the presence of either PVP or BSA increased the enzyme activity to 22 and 37 % respectively. The molar ratio of BSA and PVP to 3,4,5 tri-*O*-galloylquinic acid was 5:1 and 8:1 respectively,. The binding of 3,4,5 tri-*O*-galloylquinic acid to RT was therefore abnormally strong in comparison to 3,4,5 tri-*O*-galloylquinic acid binding to BSA and PVP.

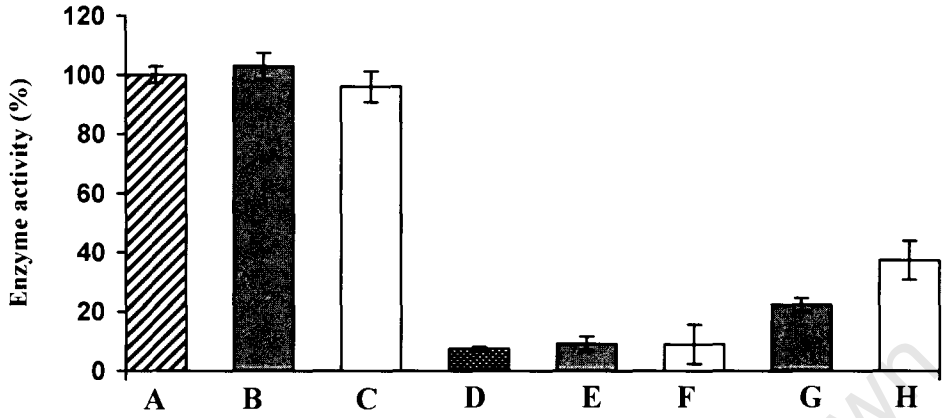

Figure 3.9: Effect of PVP and BSA on M-MLV RT activity in the absence and presence of 0.9 µM 3,4,5 tri-*O*-galloylquinic acid.

The enzyme activity assay was performed as follows: (A) no addition,; (B) PVP; (C) BSA; (D) 0.9 µM 3,4,5 tri-*O*-galloylquinic acid; (E) Enzyme + 3,4,5 tri-*O*-galloylquinic acid, then PVP; (F) Enzyme + 3,4,5 tri-*O*-galloylquinic acid, then BSA; (G) PVP + 3,4,5 tri-*O*-galloylquinic acid, then Enzyme; (H) BSA + 3,4,5 tri-*O*-galloylquinic acid, then Enzyme. The data represent the mean (± SD) of three replicate samples.

It has been reported that the type and strength of the interaction between polyphenols and proteins is influenced by their functional groups (Hagerman, 2002). The hydroxyl groups on the galloyl moiety are thought to play a crucial role in the interaction of galloyl-containing polyphenols with proteins (Kawamoto et al., 1995). Phenylalanine and proline residues have been considered to be the polyphenol binding sites on the protein (Charlton et al., 2002) and it has been reported that the polyphenol affinity for protein was dependent on the proline content (Hagerman and Butler, 1981). Although the total phenylalanine and proline contents of the BSA and M-MLV RT are similar at 10.2 and 10.6 mol % respectively, BSA has significantly higher phenylalanine content whereas M-MLV RT has significantly higher proline content. Whereas phenylalanine is a

hydrophobic amino acid with a hydropathy index of 2.8, proline is a hydrophilic amino acid with a hydropathy index of -1.6 (Kyte and Doolittle, 1982). Thus phenylalanine residues would tend to be buried in most proteins (Charlton et al., 2002), leaving proline as the only effective polyphenol binding site. This is a possible reason why 3,4,5 tri-*O*-galloylquinic acid binding to M-MLV RT was significantly stronger than to BSA.

Table 3.4: A comparison of the phenylalanine and proline contents of BSA and M-MLV RT

	Content (mol %)	
Protein	**Proline**	**Phenylalanine**
BSA	4.8	5.4
M-MLV RT	8.0	2.6

3.4.6 Effect of Nevirapine on M-MLV RT activity

Nevirapine, a derivative of dipyridodiazepinone, is a non-nucleoside reverse transcriptase inhibitor widely used in the prevention of mother to child HIV transmission. It has been shown to bind to HIV-1 RT non-competitively, resulting in disruption of the enzyme catalytic site (Riska et al., 1999). Nevirapine was dissolved in 40 % DMSO and its effect on M-MLV RT activity was investigated using different concentrations up to 1.0 mM. No effect was observed either for Nevirapine or for DMSO alone used as a control. Nevirapine has been reported to be a highly specific HIV-1 RT inhibitor but ineffective against HIV-2 and other RTs from simian immunodeficiency and feline leukemia viruses

(Smerdon et al., 1994; Merluzzi et al., 1990). This specificity could account for its inactivity against M-MLV RT even at concentrations ten times higher than the IC_{50} for 3,4,5 tri-*O*-galloylquinic acid

3.5 Enzymology of HIV-1 Reverse Transcriptase

3.5.1 Effect of substrate concentration on HIV-1 RT activity

A plot of the initial velocity (V_o) against the substrate concentration for HIV-1 RT showed that an increased reaction rate occurred as a function of the dTTP concentration. This rate reached a maximum at 0.25 mM dTTP (Figure 3.10). Further addition of dTTP resulted in a gradual decrease in the rate of cDNA synthesis. Inhibition of HIV-1 RT was most likely due to substrate inhibition and not Mg^{2+} depletion, since the Mg^{2+} concentration used was 5 mM.

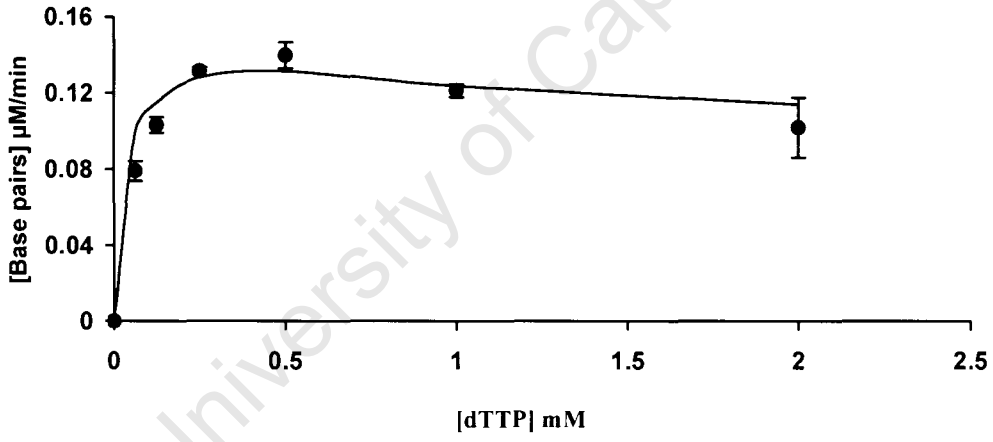

Figure 3.10: Initial rate (Vo) for the formation of cDNA as a function of the dTTP concentration.

The assay was carried out in the presence of 5.0 mM $MgCl_2$. The data represent the mean (± SD) of two replicate samples.

The kinetic parameters of the reaction were estimated using a model that accounts for data that exhibit substrate inhibition (Cleland, 1979). It is based on the assumption (Verhamme et al., 1988) that an ineffective (dead end) enzyme substrate complex with two substrate molecules (ESS_i) is formed as shown below (a):

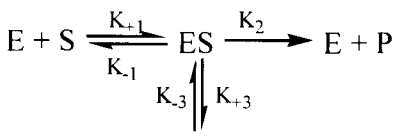

(a)

The rate equation (b) is derived from the reaction scheme (a) above.

$$V = \frac{V_{max}[S]}{K_m + [S] + ([S]^n/K_i)} \qquad (b)$$

The data for the initial rate of cDNA formation as a function of dTTP fitted well when n was assigned a value of 2, suggesting that the model reasonably described the kinetics of HIV-1 RT as the concentration of dTTP increased. The superscript "n" represented the total number of substrate molecules bound to an ineffective complex. Since two substrate molecules were bound to the enzyme, K_i was given by the equation below (c):

$$K_i = \frac{[ES][S]}{[ESS_i]} \qquad (c)$$

The K_m, K_i and V_{max} were estimated to be 0.097 ± 0.004 mM, 10.82 ± 1.20 mM and 0.223 ± 0.004 μM/min respectively. The data were further analysed using a Hill plot to assess if the binding of the first dTTP molecule to HIV-RT had an effect on the binding of the second molecule. A Hill coefficient of one was obtained at low dTTP concentration and less than one at high dTTP concentration, suggesting zero and negative cooperativity respectively (Michel, 2007).

Failure by HIV-1 RT to obey Michaelis – Menten kinetics has been reported previously (Furman et al., 1991). These authors used a recombinant HIV-1 RT to incorporate dTTP into a poly (rA).oligo(dT_{10}) complex. Substrate inhibition was reported to occur at concentrations above 50 μM dTTP and the reported K_i was 195 ± 37 μM.

3.5.2 Effect of 3,4,5 tri-*O*-galloylquinic acid on HIV-1 RT activity

Since 3,4,5 tri-*O*-galloylquinic acid inhibited M-MLV RT activity, an assay was performed to assess whether a similar inhibition was observed with HIV-1 RT. The concentrations of 3,4,5 tri-*O*-galloylquinic acid used were up to 82 µM. The results showed an exponential response of HIV-1 RT inhibition in this concentration range (Figure 3.11) and the IC_{50} was estimated to be 34 µM. A similar IC_{50} value for 3,4,5 tri-*O*-galloylquinic acid inhibition of HIV-1 RT has been reported previously using an enzyme activity assay based on the incorporation of radio-labeled [^{3}H] dTMP into poly(rA).oligo(dT)$_{25}$ complex (Nishizawa et al., 1989).

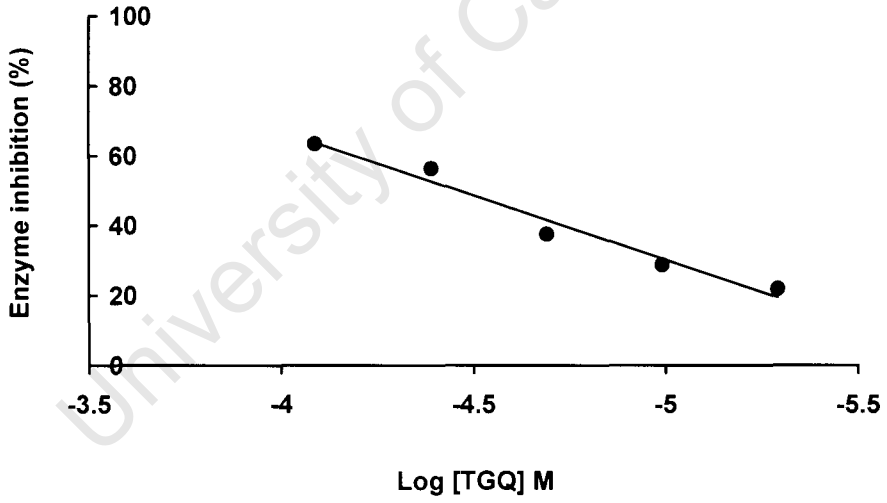

Figure 3.11: Inhibition of HIV-1 RT activity as a function of 3,4,5 tri-O-galloylquinic acid concentration.

The data shown represent a single value. Replicate values were not performed due to the high cost of HIV-1 RT

3.5.3 Mode of 3,4,5 tri-*O*-galloylquinic acid binding to HIV-1 RT

The nature of HIV-1 RT inhibition by 3,4,5 tri-*O*-galloylquinic acid was investigated by assaying HIV-1 RT activity in the presence and absence of 34 μM 3,4,5 tri-*O*-galloylquinic acid. The Mg^{2+} concentration used was 5.0 mM.

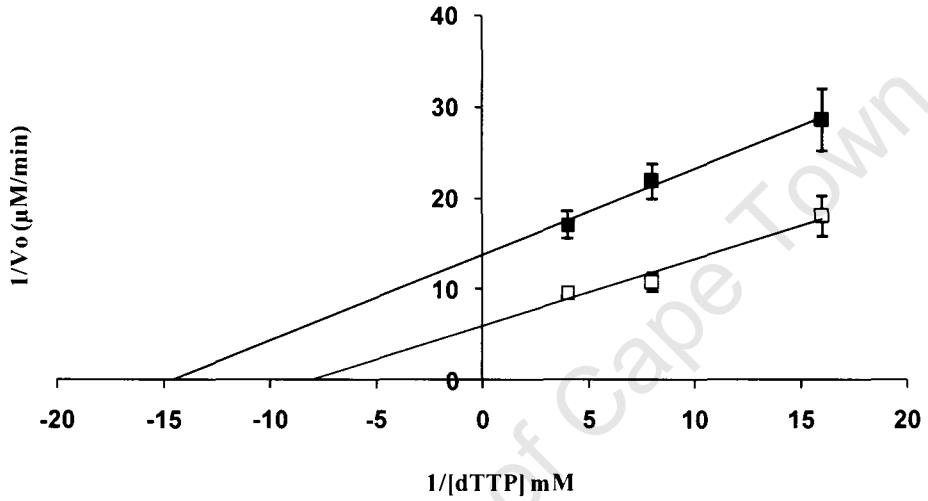

Figure 3.12: Lineweaver-Burk plot of dTTP incorporation into poly (rA).oligo(dT)$_{25}$ by HIV-1 RT in the presence (■) and absence (□) of 34 μM 3,4,5 tri-*O*-galloylquinic acid.

The data represent the mean (± SD) of two replicate samples.

A Lineweaver-Burke plot (Figure 3.12) showed an apparent change in the values of both the K_m and V_{max} in the presence of 3,4,5 tri-*O*-galloylquinic acid. This suggested mixed non-competitive inhibition. This type of inhibition demonstrated that 3,4,5 tri-*O*-galloylquinic acid bound HIV-1 RT at a site other than the active site, and also that its binding influenced the binding of dTTP. It has been reported that non-nucleoside HIV-1 RT inhibitors (NNRTI's) such as Nevirapine, Efivarenz and Delaviridine, bind to the same hydrophobic pocket that is located between the β-sheets of the palm and the base of the thumb sub-domains, near the active site

(Kohlstaedt et al., 1992, Pata et al., 2004). It is possible that 3,4,5 tri-*O*-galloylquinic acid binds to this same NNRTI hydrophobic pocket. Mixed non-competitive inhibition has, however, been reported to occur if the binding sites for both substrate and inhibitor are in close proximity or if the binding of inhibitor induces a conformational change in the enzyme which affects substrate binding (Garrett and Grisham, 2005). Inhibition constants for mixed non-competitive inhibition are not the same, i.e. $K'_i \neq K_i$. In the case of inhibition of HIV-1 RT by 3,4,5 tri-*O*-galloylquinic acid, the value of K'_i was less than that of K_i suggesting that binding of 3,4,5 tri-*O*-galloylquinic acid to the enzyme substrate complex (ES) was stronger than to the free enzyme (E). Kinetic parameters for dTTP incorporation into poly (rA).oligo(dT25) complex by HIV-1 RT in the absence and presence of 3,4,5 tri-*O*-galloylquinic acid are summarized in Table 3.5. The V_{max} and Km values observed were similar to those estimated previously (Figure 3.10)

Table 3.5: Kinetic parameters for dTTP incorporation into poly (rA) : oligo $(dT)_{25}$ complex using HIV-1 RT in the presence and absence of 3,4,5 tri-*O*-galloylquinic acid.

Reaction velocity units represent the concentration of base pairs incorporated per minute

Parameter		No TGQ added	TGQ added
V_{max}	(μM/min)	0.169 ± 0.002	
V'_{max}	(μM/min)		0.072 ± 0.004
K_m	(mM)	0.13 ± 0.03	
K'_m	(mM)		0.07 ± 0.01
K_i	(μM)		135 ± 89
K'_i	(μM)		26 ± 2

3.5.4 Reversibility of 3,4,5 tri-*O*-galloylquinic acid binding to HIV-1 RT

The reversibility of 3,4,5 tri-*O*-galloylquinic acid binding to M-MLV RT was determined by performing an enzyme activity assay in the presence of 100 μM 3,4,5 tri-*O*-galloylquinic acid and 11.0 μM BSA. The BSA molar concentration was sufficient to bind all the 3,4,5 tri-*O*-galloylquinic acid present (Kawamoto et al, 1995). The molar ratio of BSA to HIV-1 RT was 63:1. The Mg^{2+} concentration was 5.0 mM. The results showed that HIV-1 RT activity in the presence of BSA alone was similar to that in its absence (Figure 3.13), showing that BSA did not inhibit HIV-1 RT activity. The activity of the enzyme in the presence of 3,4,5 tri-*O*-galloylquinic acid alone was approximately 5 %. BSA addition subsequent to 3,4,5 tri-*O*-galloylquinic acid addition restored the activity of HIV-1 RT to 53 %. Similarly, HIV-1 RT addition subsequent to BSA and 3,4,5 tri-*O*-galloylquinic acid addition resulted in an activity of 63 %, clearly showing that the binding of 3,4,5 tri-*O*-galloylquinic acid to HIV-1 RT was reversible.

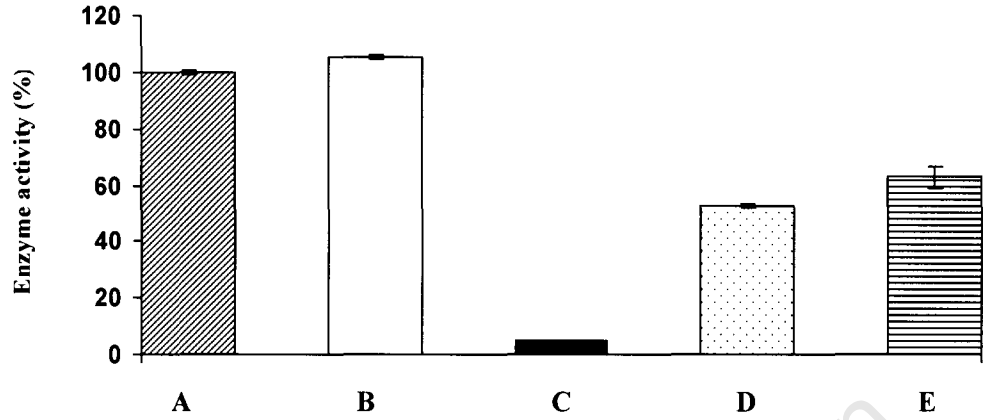

Figure 3.13: Effect of BSA on HIV-1 RT activity in the absence and presence of 100 µM 3,4,5 tri-*O*-galloylquinic acid

The enzyme activity was performed as follows: (A) no addition; (B) BSA; (C) 100 µM 3,4,5 tri-*O*-galloylquinic acid; (D) HIV-1 RT + 3,4,5 tri-*O*-galloylquinic acid, then BSA; (E) BSA + 3,4,5 tri-*O*-galloylquinic acid, then HIV-1 RT. The data represent the mean (±SD) of duplicate samples

3.5.5 Effect of Nevirapine on HIV-1 RT

The effect of Nevirapine on HIV-1 RT activity was next investigated. The results showed that addition of Nevirapine to the RT assay at 1 µM caused double the inhibition observed at 100 nM (Table 3.6), but that the higher concentration was insufficient to reduce the activity by 50 %. No effect was observed for DMSO alone used as a control. Although the median 50 % inhibitory concentration for Nevirapine has been reported to be 100 nM (Merluzzi et al., 1990), this study was performed using a RT from a different HIV strain. Since Nevirapine has been reported to interact with Tyr 181 and Tyr 188 residues in the inhibitor binding pocket of HIV-RT through aromatic ring stacking, any mutation at either of these two residues would result in reduced Nevirapine binding. Moreover, a wide range of single point mutations in HIV-1 RT has been associated with HIV-1 RT resistance to Nevirapine (Kohlstaedt et, 1992, Ren et al, 2001, 2004)

Table 3.6: Effect of Nevirapine on HIV-1 RT activity

[Nevirapine]	Inhibition (%)
100 nM	14 ± 2
1 μM	31 ± 6

3.6 A comparison of the catalytic efficiencies of M-MLV RT and HIV-1 RT and their response to 3,4,5 tri-*O*-galloylquinic acid

3.6.1 Catalytic efficiencies

The kinetic parameters for the two RTs were compared (Table 3.7). Since the concentrations of M-MLV and HIV-1 RT used were 0.071 μM and 0.17 μM respectively, V_{max} could not be used to compare the efficiencies since it is dependent on the initial enzyme concentration. K_{cat} and K_m, however, are independent of the initial enzyme concentration, and so can be used to compare catalytic efficiencies.

K_{cat} (the turnover number or molecular activity) is the number of substrate molecules converted into product per enzyme molecule per unit time under saturating substrate conditions. The kinetic efficiency of a given enzyme is directly proportional to the turnover number (Garrett and Grisham, 2005). The turnover number of M-MLV RT was approximately 10 times higher than that of HIV-1 RT (Table 3.7). K_{cat} has been reported to be physiologically irrelevant, because substrates rarely attain saturating concentrations *in vivo*. The kinetic efficiency under physiological conditions is therefore given by an apparent second order rate constant, K_{cat}/K_m (Garrett and Grisham, 2005), which was similar for both enzymes. These findings demonstrated that M-MLV RT was kinetically more efficient than HIV-1 RT under saturating substrate concentrations, and equally efficient under limiting substrate concentrations. K_m is the concentration of the substrate that results in the velocity of an enzymatic reaction equal to half its maximum velocity, and its value varies inversely with the strength of binding between substrate

and enzyme (Garrett and Grisham, 2005). Results showed stronger binding of dTTP to HIV-1 RT than to M-MLV RT.

Table 3.7: Kinetic parameters for cDNA synthesis by M-MLV and HIV-1 RTs.

The K_m value is an average of K_m values from two independent experiments

Parameter	Enzyme	
	M-MLV RT	HIV-1 RT
V_{max} (M/min)	$0.8 \pm 0.2 \times 10^{-6}$	$0.22 \pm 0.004 \times 10^{-6}$
K_{cat} (min^{-1})	11 ± 3	1.31 ± 0.02
K_m (M)	$0.98 \pm 0.14 \times 10^{-3}$	$0.11 \pm 0.015 \times 10^{-3}$
K_{cat}/K_m ($min^{-1}M^{-1}$)	$1.1 \pm 0.3 \times 10^{4}$	$1.2 \pm 0.2 \times 10^{4}$

3.6.2 Response to 3,4,5 tri-*O*-galloylquinic acid

The dose response curves for HIV-1 RT and M-MLV RT activity as a function of the 3,4,5 tri-*O*-galloylquinic acid concentration are compared in Figure 3.14. Both enzymes showed decreased catalytic activity in the presence of 3,4,5 tri-*O*-galloylquinic acid. The IC_{50} values were 0.5 µM and 34 µM for M-MLV RT and for HIV-1 RT respectively, this occurring at molar ratios of 3,4,5 tri-*O*-galloylquinic acid:M-MLV RT and 3,4,5 tri-*O*-galloylquinic acid:HIV-1 RT of 7:1 and 200:1 respectively. This was a clear indication that M-MLV RT was very much more sensitive to 3,4,5 tri-*O*-galloylquinic acid than HIV-1 RT. 3,4,5 Tri-*O*-galloylquinic acid inhibited M-MLV and HIV-1 RT activities by binding at an allosteric site. Whereas inhibition was purely non-competitive for

M-MLV RT, mixed non-competitive inhibition was observed for HIV-1 RT. 3,4,5 Tri-*O*-galloylquinic acid binding to M-MLV RT was irreversible, which suggested strong interactions. Weak interactions, however, existed between 3,4,5 tri-*O*-galloylquinic acid and HIV-1 RT as the activity of the enzyme was partially restored on subsequent addition of BSA to the HIV-1 RT -3,4,5 tri-*O*-galloylquinic acid mixture.

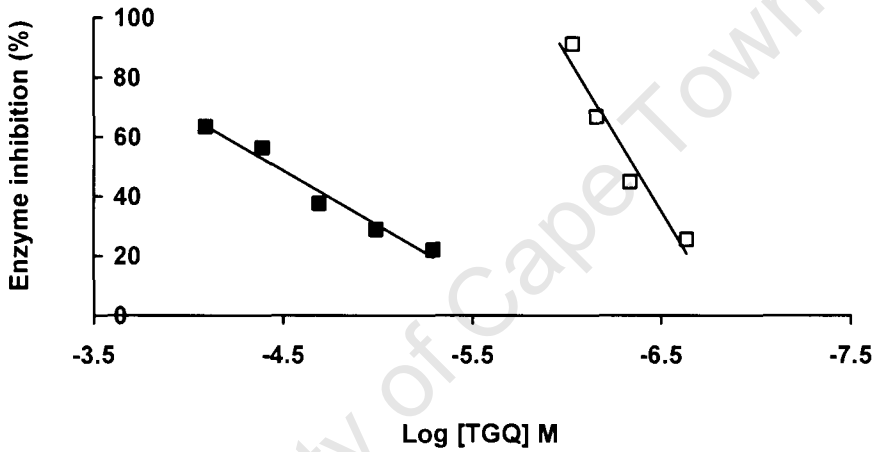

Figure 3.14: 3,4,5 tri-*O*-galloylquinic acid inhibition of HIV-1 RT (■) and M-MLV RT (□) activity

CONCLUSION

A quick, reliable non-radioactive reverse transcriptase assay was developed. This was used to confirm the previous finding that the HIV-1 RT enzyme displayed substrate inhibition (Furman et al., 1991). This assay was also used to confirm the IC_{50} for 3,4,5 tri-*O*-galloylquinic acid inhibition of HIV-1 RT (Nishizawa et al., 1988) as well as Nevirapine specificity for HIV-1 RT inhibition (Merluzzi et al., 1990; Smerdon et al., 1994).

Although the M-MLV and HIV-1 RT enzymes belong to the same family, they differ in their responses to treatment with inhibitors. Thus 3,4,5 tri-*O*-galloylquinic acid non-competitively inhibited M-MLV RT whereas mixed inhibition was observed for HIV-1 RT under similar conditions. The IC_{50} values for 3,4,5 tri-*O*-galloylquinic acid were also different, with M-MLV RT being more sensitive to this compound than HIV-1 RT. Care therefore needs to be taken in postulating the kinetic behaviour of a given RT enzyme since it may not be representative of the RT family.

The data regarding HIV-1 RT inhibition by 3,4,5 tri-*O*-galloylquinic acid suggested that it would be highly unlikely that oral administration of this polyphenol would act as an effective inhibitor of HIV reverse transcriptase for the following reasons:

1. The relatively high concentration (IC_{50}= 34 μM) of 3,4,5 tri-*O*-galloylquinic acid required to inhibit the HIV RT would necessitate ingestion of large quantities of this polyphenol since only relatively small amounts of free and

glycosylated polyphenols are absorbed into the blood stream (Conquer et al., 1997, Neuhouser, 2004) .

2. The competitive and non specific binding of 3,4,5 tri-*O*-galloylquinic acid to other proteins such as serum albumin would reduce the effective concentration of this polyphenol in the blood stream.
3. The 3,4,5 tri-*O*-galloylquinic acid concentration inside the appropriate immune cell would most likely be substantially lower than that in the blood stream due to transport constraints.

However, preliminary results have shown that 3,4,5 tri-*O*-galloylquinic acid reduces the viral count in tissue culture experiments (Brandt, unpublished results). It would appear this polyphenol reduces the entry of HIV-1 into CD-4 cells. This could be due to the binding of 3,4,5 tri-*O*-galloylquinic acid to the viral coat proteins or to interacting with the cell membrane and/or membrane proteins. This may explain why healthy nutrition and the incorporation of fruits and vegetables into the diet lowers the HIV viral count in HIV-infected individuals.

REFERENCES

Amarowicz, R., Kolodziejczyk, P., Pegg, R., 2003. Chromatographic separation of phenolic compounds from rapeseed by a Sephadex LH-20 column with ethanol as the mobile phase. *Journal of liquid chromatography and related technologies.* 26: 2157-2165.

Baser, K., Van Wyk, B., 2002. The composition and antimicrobial activity of the essential oil of the resurrection plant *Myrothamnus flabellifolius*. *South African Journal of Botany.* 66: 100-105.

Bennick, A., 2002. Interaction of plant polyphenols with salivary proteins. *Critical Review in Oral Biology and Medicine.* 13: 184-196.

Bokesh, H., McKee, T., Currens, M., Gulakowski, R., Mcmahon, J., Cardellina, J., Boyd, M., 1996. HIV-Inhibitory Gallotannins from *Lepidobotrys staudtii*. *Natural Product Letters.* 8: 133-136.

Carbonaro, M., Virgili, F., Carnovale, E., 1996. Evidence for protein-tannin interaction in legumes: Implications in antioxidant properties of *Faba* bean tannins. *Lebensmittel-Wissenschaft und Technologie.* 29:743-750.

Charlton, A., Baxter, N., Khan, M., Moir, A., Haslam, E., Davies, A., Williamson, M., 2002. Polyphenol/peptide binding and precipitation. *Journal of Agricultural and Food Chemistry.* 50:1593-1601.

Chen, Y., Hagerman, A., 2004. Quantitative examination of oxidised polyphenol-protein complexes. *Journal of Agricultural and Food Chemistry*. 52: 6061-6067.

Cleland, W., 1979. Statistical analysis of enzyme kinetic data. *Methods in enzymology*. 63: 103-138.

Conquer, J., Maian, G., Azzini, E., Raguzzini, A., Holub, B., 1998. Supplementation with quercetin markedly increases plasma quercetin concentration without effect on selected risk factors for heart disease in healthy subjects. *The Journal of Nutrition*. 128: 593-597.

Cushman, D., Ondetti, M., 1995. Designing of angiotensin converting enzyme inhibitors. *Nature Medicine*. 5: 1110 - 1112

Das, D., Georgiadis, M., 2004. The crystal structure of the monomeric reverse transcriptase from Molony Murine Leukemia Virus. *Structure*. 12: 819-829.

Dixon, M., Webb, C., 1979. In *Enzymes*. Longman Group Limited, London. 3: 133.

Escribano-Bailon M., Santos-Buelga C., 2003. In *Methods in plant polyphenol analysis* (ed: Santos-Buelga C and Williamson G). The Royal Society of Chemistry, United Kingdom. 1-16

Fisher, T., Joshi, P., Prasad, V., 2005. HIV-1 reverse transcriptase mutations that confer decreased in vitro susceptibility to anti- RT DNA aptamer RTIt49 (confer cross resistance to other anti-RT aptamers but not to standard RT inhibitors. *AIDS Research and Therapy*. 2;8 doi: 10.1186/1742-6405-2-8.

Furman, P., Painter, G., Wilson, J., Cheng, N., Hopkins, S., 1991. Substrate inhibition of the human immunodeficiency virus type type 1 reverse transcriptase. *Procceedings of the National Academy of Sciences.* 88: 6013-6017.

Garbett, N., Hammond, N., Graves, D., 2004. Influence of the amino substituents in the interaction of ethidium bromide with DNA. *Biophysical Journal.* 87: 3974-3981

Garrett, R., Grisham, C., 2005. In *Biochemistry.* Thomson Brooks/Cole, USA/Australia/Canada. 3: 412-424.

Goldschmidt, V., Didierjean, J., Ehresmann, B., Ehresmann, C., Isel, C., Marquet, R., 2006. Mg^{2+} dependency of HIV-1 reverse transcription, inhibition by nucleoside analogues and resistance. *Nucleic Acids Research.* 34: 42-52.

Hagerman, A., 2002. Tannin Chemistry. Available from URL: http://www.users.muohio.edu/hagermae/tannin.pdf

Hagerman, A., Butler, L., 1981. The specificity of proanthocyanidin-protein interactions. *The Journal of Biological Chemistry.* 256: 4494-4497.

Huang, H., Chopra, R., Verdine, G., Harrison, S., 1998. Structure of a covalently trapped catalytic complex of HIV-1 reverse transcriptase: Implications for drug resistance. *Science.*282: 1669-1675.

Kantz, K., Singleton, V., 1990. Isolation and determination of polymeric polyphenols using Sephadex LH-20 and analysis of grape tissue extracts. *American Journal of Enology and Viticulture.* 41: 223-228.

Kawamoto, H., Nakatsubo, F., Murakami, K., 1996. Stoichiometric studies of tannin-protein co-precipitation. *Phytochemistry*. 41: 1427-1431.

Khan, N., Mukhtar, H., 2007. Tea polyphenols for health promotion. *Life Sciences*. 81: 519-533.

Kohlstaedt, L., Wang, J., Friedman, J., Rice, P., Steitz, T., 1992. Crystal structure at 3.5 Å resolution of HIV-1 Reverse Transcriptase complexed with an inhibitor. *Science*. 256: 1783-1790.

Koonjul, P., Brandt, W., Farrant, J., Lindsey, G., 1999. Inclusion of polyvinylpyrrolidone in the polymerase chain reaction reverses the inhibitory effects of polyphenolic contamination of RNA. *Nucleic Acids Research*. 27: 915-916.

Kuhl, P., 1994. Excess-substrate inhibition in enzymology and high-dose inhibition in pharmacology: a re-interpretation. *Biochemical Journal*. 298:171-180.

Kyte, J., Doolittle, R., 1982. A simple method for displaying the hydropathic character of a protein. *Journal of Molecular Biology*. 157: 105-132.

Lanchy, J., Ehresmann, C., Grice, S., Ehresmann, B., Marquet, R., 1996. Binding and kinetic properties of HIV-1 reverse transcriptase markedly differ during initiation and elongation of reverse transcription. *The EMBO Journal*. 15: 7178-7187.

Lin, Y., Lu, P., Tang, C., Mei, Q., Sandig, G., Rodrigues, D., Rushmore, T., Shou, M., 2001. Substrate inhibition kinetics for cytochrome P450-catalysed reactions. *Drug metabolism and disposition*. 29: 368-374.

Maggi, M., Filippi, S., Ledda, F., Magini, A., Forti, G., 2000. Erectile dysfunction: from biochemical pharmacology to advances in medical therapy. *European Journal of Endocrinology*. 143:143-154.

Makkar, H., Bluemmel, M., Borowy, N., Becker, K., 1993. Gravimetric determination of tannins and their correlations with chemical and protein precipitation methods. *Journal of Science and Food Agriculture*. 61: 161-165.

Makkar, H., 2003. In Quantification of tannins in tree and shrub foliage: A laboratory manual. Kluwer academic publishers. Doldrecht/Boston/London. 50-51.

Marchand, C., Johnson, A., Semenova, E., Pommier, Y., 2006. Mechanisms and inhibition of HIV integration. *Drug Discovery Today: Disease Mechanisms*. 3: 253-260.

Merluzzi, J., Hargrave, K., Labadia, M., Grozinger, K., Skoog, M., Wu, J., Shih, C., Eckner, K., Hattox, S., Adams, J., Rosehthal, A., Faanes, R., Eckner, R., Koup, R., Sullivan, J., 1990. Inhibition of HIV-1 replication by a nonnucleoside reverse transcriptase inhibitor. *Science*.250: 1411-1413.

Michel, D., 2007. Cooperative equilibrium curves generated by ordered ligand binding to multi-site molecules. *Biophysical Chemistry*. 129: 284-288.

Minasyan, S., Tavadyn, L., Antonyan, A., Davtyan, H., Parsadanyan, M., Vardervanyan, P., 2006. Differential pulse voltametric studies of ethidium bromide binding to DNA. *Biochemistry*. 68: 48-55.

Moore, J., Farrant, J., Lindsey, G., Brandt, W., 2005a. The South African and Namibian populations of the resurrection plant Myrothamnus flabellifoli are genetically distinct and display variation in their galloylquinic acid composition. *Journal of Chemical Ecology*. 31: 2823-2834.

Moore, J., Lindsey, G., Farrant, J., Brandt, W., 2007. An overview of the biology of the desiccation – tolerant resurrection plant Myrothamnus flabellifolia. *Annals of Botany*. 211 – 217.

Moore, J., Westall, K., Ravenscroft, N., Farrant, J., Lindsey, G., Brandt, W., 2005b. The predominant polyphenol in the leaves of the resurrection plant *Myrothamnus flabellifolius*, 3, 4, 5 tri-O-galloylquinic acid, protects membranes against desiccation and free radical-induced oxidation. *Biochemical Journal*. 385: 301-308.

Mozetic, B., Tomazic, I., Skvarc, A., Trebse, P., 2006. Determination of polyphenols in white grape berries cv. *Rebula. Acta Chimica Slovenica*. 53: 58-64.

Murray, N., Williamson, M., Lilley, T., Haslam, E., 1994. Study of the interaction between salivary proline-rich proteins and a polyphenol by ^{1}H-NMR spectroscopy. *European Journal of Biochemistry*. 219: 923 - 935

Neuhouser, M., 2004. Dietary flavonoids and cancer risk: Evidence from human population studies. *Nutrition and Cancer*. **50: 1-7.**

Nishizawa, M., Yamagishi, T., Dutschman, G., Parker, W., Bodner, A., Kilkuskie, R., Cheng, Y., Lee, K., 1989. Anti–Aids agents. 1. Isolation and characterisation of four new tetragalloylquinic acids as a new class of HIV reverse transcriptase inhibitors from tannic acid. *Journal of Natural Products*. 52: 762-768.

Nomura, D., Leung, D., Chiang, K., Quistad, G., Cravatt, B., Casida, J., 2005. A brain detoxifying enzyme for organophosphorus nerve poisons. *Procceedings of the National Academy of Sciences.* 102: 6195 - 6200

Notka, F., Meier, G., Wagner, R., 2004. Concerted inhibitory activities of *Phyllanthus amarus* on HIV replication in vitro and ex vivo. *Antiviral Research*. 64: 93-102.

Oelschlaeger, P., Klahn, M., Beard, A., Wilson, S., Warshel, A., 2007. Magnesium-cationic dummy atom molecules enhance representation of DNA polymerase β in molecular dynamics simulations: Improved accuracy in studies of structural features and mutational effects. *Journal of Molecular Biology*. 366: 687-701.

Oliver, C., Shenolikar, S., 1998. Physiologic importance of protein phosphatase inhibitors. *Frontiers in Bioscience*. 3: D961 – 972.

Pata, J., Stirtan, W., Golgstein, S., Steitz, T., 2004. Structure of HIV-1 reverse transcriptase bound to an inhibitor active against mutant reverse transcriptases resistant to other nonnucleoside inhibitors. *Proceedings of the National Academy of Sciences*. 101: 10548-10553.

Pelemans, H., Esnouf, R., De Clercq, E., Balzarini, J., 2000. Mutational analysis of Trp-229 of Human Immunodeficiency Virus Type 1 Reverses Transcriptase (RT) identifies this amino acid residue as a prime target for the rational design of new non-nucleoside RT inhibitors. *Molecular Pharmacology*. 57: 954-960.

Reed, J., Krueger, C., Vestling M., 2005. MALDI-TOF mass spectrometry of oligomeric food polyphenols. *Phytochemistry*.66: 2248-2263.

Reha, D., Kabelac, M., Ryjacek, F., Sponer, J., Sponer, J., Elstner, M., Suhai, S., Hobza, P., 2002. Intercalators. 1. Nature of stacking interactions between intercalators (Ethidium, Daunomycin, Ellipticine, and 4, 6- Diaminide-2-phenylindole) and DNA base pairs. Ab initio quantum chemical, density functional theory, and empirical potential study. *Journal of American chemical society*. 124: 3366-3376.

Rein, D., Paglieroni, T., Pearson, D., Wun, T., Schmitz, H., Gosselin, R., Keen, C., 2000. Cocoa and wine polyphenols modulate platelet activation and function. *The Journal of Nutrition*. 130: 2120S-2126S.

Ren, J., Nichols, C., Bird, L., Chamberlain, P., Weaver, K., Short, S., Stuart, D., Stammers, D., 2001. Structural mechanisms of drug resistance for mutations at codons 181 and 188 in HIV-1 Reverse Transcriptase and the improved resilience of second generation non-nucleoside inhibitors. *Journal of Molecular Biology*. 312: 795-805.

Ren, J., Nichols, C., Bird, L., Chamberlain, P., Weaver, K., Short, S., Stuart, D., Stammers, D., 2004. Crystal structures of HIV-1 Reverse Transcriptase mutated at codons 100. 106 and 108 and mechanisms of resistance to non-nucleoside inhibitors. *Journal of Molecular Biology*. 336: 569-567.

Ren, J., Stammers, D., 2005. HIV reverse transcriptase structures: designing new inhibitors and understanding mechanisms of drug resistance. *Trends in Pharmacological Sciences*. 26: 4-7.

Riska, P., Lamson, M., MacGregor, T., Sabo, J., Hattox, S., Pav, J., Keirns, J., 1999. Disposition and biotransformation of antiretroviral drug nevirapine in humans. *Drug Metabolism and Disposition.* 27: 895-901.

Sarafianos, S., Kortz, U., Pope, M., Modak, M., 1996. Mechanism of polyoxometalate-mediated inactivation of DNA polymerases: an analysis with HIV-1 reverse transcriptase indicates specificity for the DNA-binding cleft. *Biochemical Journal*. 319: 619-626.

Scalbert, A., Williamson, G., 2000. Dietary intake and bioavailability of polyphenols. *Journal of Nutrition.* 130: 2073S-2085S.

Seger, C., Eberhart, K., Sturm, S., Strasser, H., Stuppner, H., 2006. Apolar chromatography on Sephadex LH-20 combined with high-speed counter-current chromatography, High yield strategy for structurally closely related analytes-Destruxin derivatives from *Metarhizium anisopliae* as a case study. *Journal of Chromatography A*. 1117: 67-73.

Sherwin, H., Pammenter, H., February, E., Willingen, C., Farrant, J., 1998. Xylem hydraulic characteristics, water relations and wood anatomy of the resurrection plant *Myrothamnus flabellifolius* Welw. *Annals of Botany*.81: 567-575.

Shen, P., Larter, R., 1994. Role of substrate inhibition kinetics in enzymatic chemical oscillations. *Biophysical Journal*. 67: 1414-1428.

Shrikhande, A., 2000. Wine by-products with health benefits. *Food Research International*. 33: 469-474.

Sischka, A., Toensing, K., Eckel, R., Wilking, S., Sewald, N., Ros, R., Anselmetti, D., 2005. Molecular mechanisms and kinetics between DNA and DNA binding ligands. *Biophysical Journal*. 88: 404-411.

Smerdon, S., Jager, J., Wang, J., Kohlaestaedt, L., Chirino, A., Friedman, J., Rice, P., Steitz, T., 1994. Structure of the binding site for nonnucleoside inhibitors of the reverse transcriptase of human immunodeficiency virus type 1. *Proceedings of the National Academy of Sciences*. 91: 3911-3915.

Sovak, M., 2001. Grape extract, Resveratrol and its analogs: A review. *Journal of medicinal food*. 4: 93 – 105.

Stryer, L., 1995. In *Biochemistry*. WH Freeman and Company, New York. 4: 189.

Szedlacsek, S., Duggleby, R., 1995. Kinetics of slow and tight-binding inhibitors. *Methods in Enzymology*. 249: 144-180.

Telesnitsky, A., Goff, S., 1993. Two defective forms of reverse transcriptase can complement to retroviral infectivity. *The EMBO Journal.* 12: 4433 – 4438.

Van Wyk, B., Gericke, N., 2000. In *People's plants.* Briza Publications, Pretoria. 1: 108, 190, 210.

Verhamme, I., Van Dedem, G., Lauwers, A., 1988. Ionic-strength-dependent substrate inhibition of the lysis of Micrococcus luteus by hen egg-white lysozyme. *European Journal of Biochemistry.* 172: 615-620.

Vicre, M., Farrant, J., Gibuon, D., Drouich, A., 2003. Resurrection plant: How to cope with desiccation. *Recent Research Development in Plant Biology.* 3: 69-93.

Viljoen, A., Klepser, M., Ernst, E., Keele, D., Roling, E., Van Vuuren, S., Demicri, B., Baser, K., Van Wyk, B., 2002. The composition and antimicrobial activity of the essential oil of the resurrection plant *Myrothamnus flabellifolius. South African Journal of Botany.* 66: 100-105.

Whiteley, C., 2000. Mechanistic and kinetic studies of Inhibition of enzymes. *Cell Biochemistry and Biophysics.* 33: 217-225.

Yang, L., Arora, K., Beard, A., Wilson, S., Schlick, T., 2004. Critical role of magnesium ions in DNA polymerase β's closing and active site assembly. *Journal of American Chemical Society.* 126: 8441-8453.